Geometrically exact bifurcation and post-buckling analysis of the granular elastica

Noël Challamel, Attila Kocsis

Version of Record: https://www.sciencedirect.com/science/article/pii/S0020746221001062
Manuscript_c7f6ef1a06c7b9a08d40c1f0e2d2556c

Geometrically exact bifurcation and post-buckling analysis of the granular *elastica*

Noël CHALLAMEL

Université de Bretagne Sud,

Institut de Recherche Dupuy de Lôme (IRDL), Centre de Recherche

Rue de Saint Maudé – BP 92116

F-56100 Lorient, France

(E-mail: noel.challamel@univ-ubs.fr)

and

Attila KOCSIS

Budapest University of Technology and Economics

1103 Budapest, Hungary

(Email: attila.kocsis@edu.bme.hu)

Currently independent researcher, 3800 Sint-Truiden, Belgium

Abstract :

The nonlinear behavior of a simply supported granular column loaded by an axial force is studied in this paper. The granular column is composed of rigid grains (disks) elastically connected by some shear and rotational springs. The in-plane buckling and post-buckling analysis in a geometrically exact framework is numerically investigated from a nonlinear difference eigenvalue problem. The granular column asymptotically behaves as an Engesser-Timoshenko column for a sufficiently large number of grains. An exact analytical solution of the buckling load of this discrete shear granular system is obtained from the linearization of the granular elastica problem. An asymptotic expansion is applied to the difference eigenvalue problem, to efficiently approximate the equation of the primary post-bifurcation branch of the discrete problem. Exact analytical solutions of the post-buckling branches are also available for the granular problem with few numbers of grains. Bifurcation diagrams of the granular elastica problem composed of few grains are numerically obtained with the simplex algorithm (for an exhaustive capture of all post-bifurcation branches). It is shown that the post-buckling of this granular column reveals complex behavior similarly to the post-buckling of a generalized shear Hencky column (also called discrete Engesser elastica). Complex higher-order branches are exhibited, a phenomenon very similar to the discrete elastica problem. These branches reveal the specific nature of the discrete granular problem, as opposed to its continuum limit valid for an infinite number of grains.

Keywords: Elastica – Post-buckling – Granular model – Geometrical nonlinearity – Discrete model – Granular elastica – Simplex algorithm – Bifurcation diagram – Asymptotic expansion

1. Introduction

In this paper, the buckling and post-buckling behaviour of an axially loaded granular column is studied from analytical and numerical perspectives. The instability of such granular structure is studied in view of a better understanding of shear band formation in geomaterials, including granular media. It has been experimentally and numerically observed that curved columns of particles or grains are formed during the shear band with a key role of rotation of particles, and chain of forces. These phenomena are essential in the localization process of granular materials (Satake, 1998; Hutter and Wilmanski, 1999; Cambou et al, 2009; Andreotti et al, 2013; or Vardoulakis, 2019). The present granular discrete model explored in its full geometrically nonlinear range may contribute to a better understanding of granular instabilities in geomaterials. The granular system is composed of a finite number of uniform rigid grains with independent translational and rotational degrees-of-freedom. Shear and rotational interactions are taken into account at the interface of each grain. This nonlinear problem will be investigated in a geometrically exact framework. The nonlinear behaviour of such discrete structural systems is ruled by some nonlinear difference equations, as opposed to nonlinear differential or partial differential equations valid for continuous systems.

The idea to compute the macroscopic behaviour of granular systems by modelling each grain separately, thus leading to a large scale discrete system is quite old. This idea is also related to the possibility to investigate continuum elasticity problems based on molecular elastic interactions, as suggested by Boscovich (1763) and the French mechanicians at the beginning of the XIXth century (Navier, 1823; Cauchy, 1828 and Poisson, 1829). This question was of fundamental interest during all the XIXth century (see for instance the paper of Capecchi et al, 2010 on the history of molecular elasticity). Investigating the macroscopic behaviour of continuous media from their fundamental discrete interactions is still a stimulating research nowadays, with the development of more complex interaction laws or more sophisticated computational possibilities (Dell'Isola et al, 2020; Wang et al, 2020). Even if the basic ideas behind discrete granular media based on elementary interaction laws were probably mature before the end of the XXth century, the possibility to compute effectively the nonlinear behaviour of such discrete systems only dates from the last 70's, with the so-called Distinct Element Method, due to the availability of computational

capabilities. The Distinct Element Method (DEM) has been initiated by Cundall (1971), Serrano and Rodriguez-Ortiz (1973) and Cundall and Strack (1979). This method assumes that the grains are rigid and interact with translational and rotational elastic and inelastic connections. This method has been widely and successfully applied to a large variety of engineering cases. The response of the granular particles is computed using numerical codes initially developed in the 70's (program ESTIB of Serrano and Rodriguez-Ortiz, 1973; program BALL of Cundall and Strack, 1979, which gives birth to PFC - Particle Flow Code). The research in this field is still active, especially for bridging discrete granular systems with continuous media (see the monographs of Hutter and Wilmanski, 1999; Cambou et al, 2009; Andreotti et al, 2013; or Vardoulakis, 2019). There are still some debates about the dissipative nature of the interaction law at the elementary level (see the discussion in McNamara et al, 2008; or more recently Nicot et al, 2017 or Turco et al, 2019).

In the present paper, we will formulate the geometrically exact nonlinear difference equations of a granular structural system composed of rigid circular grains with elastic granular interactions. This system can be also viewed as the analytical formulation of a Distinct Element Method applied to granular matter (where the normal interaction is neglected in the present study). The equations of motion will be deduced from an energy formulation for this nonlinear conservative elastic system. The granular column is assumed to be loaded by some axial loads, which may cause the granular system lose stability. A similar system has been considered by Satake (1998) who also studied the buckling of a granular column with constrained shear/bending interaction laws. Satake (1998) introduced this granular chain as a paradigmatic structural model which may play a key role in the shear band formation. Satake (1998) only presented some linearized equations for the calculation of the buckling load. The geometrically nonlinear exact formulation of this granular column is given by Hunt et al (2010) or Tordesillas et al (2011) based on energy arguments. Hunt et al (2010) numerically solved the buckling and post-buckling behaviour of the granular column on Winkler elastic foundation by using a path-following continuation code. Tordesillas et al (2011) numerically investigated the effect of boundary conditions on the linearized buckling behaviour of the granular column. The paper of Tordesillas and Muthuswamy (2009) should be also mentioned regarding the elastic and inelastic instabilities of granular systems, including longitudinal and cyclic granular chains. Challamel et al (2014) obtained some closed-form solution of the buckling load of a granular system by solving a linear difference eigenvalue problem. Challamel et al (2014) also highlighted the link between this discrete

stability problem and its asymptotic continuous analogue, i.e. the Engesser-Timoshenko column (Engesser, 1891; Timoshenko and Gere, 1961). As shown by Pasternak and Mühlhaus (2005), Challamel et al (2014), Challamel et al (2020) or Massoumi et al (2021), the discrete granular column may behave as a discrete Bresse-Timoshenko beam element, both in statics and in dynamics. Challamel et al (2020) more recently reconsidered the buckling of a granular column under discrete Winkler and Pasternak elastic foundations. Challamel et al (2020) also developed a higher-order gradient-type continuous beam theory for capturing the length scale effects of the granular chain. Alternative discrete Bresse-Timoshenko systems have been recently proposed by Kocsis (2016), Kocsis et al (2017), Kocsis and Challamel (2018), Battista et al (2018) or Turco et al (2020) also in a geometrically nonlinear framework. It appears that there is a strong mathematical connection between one-dimensional granular systems and discrete beam mechanics, both in the linear and in the nonlinear ranges.

The buckling and post-buckling behaviours of the granular column are investigated in this paper, based on a geometrically exact framework. Such nonlinear problem has been numerically computed by Hunt et al (2010) or Tordesillas et al (2011) who started from an energy expression of the structural interactions. The model presented in this paper leads to exactly the same total potential energy function as used in the model of Hunt et al (2010) or Tordesillas et al (2011) without lateral supporting springs and stiff normal springs, which may be labelled as a granular *elastica* (or equivalently, a geometrically exact DEM granular column). The nonlinear difference eigenvalue problem is presented both from an energy approach and from a direct approach. We numerically solve the nonlinear difference boundary value problem with the simplex algorithm (for an exhaustive capture of all post-bifurcation branches). It is shown that the post-buckling of this granular column reveals complex behavior similarly to the post-buckling of a generalized shear Hencky column (also called discrete elastica or discrete Engesser elastica in presence of shear). An exact analytical solution of the buckling load of this discrete shear granular system is obtained from the linearization of the granular elastica problem. An asymptotic expansion method is also applied to the nonlinear difference eigenvalue problem of the granular *elastica* to approximate analytically the primary bifurcation branches of the discrete granular problem. A similar method has been successively applied to a nonlinear elastic discrete repetitive system, i.e. the Hencky discrete beam problem formulated in a geometrically exact framework, by Challamel et al (2015-a). Hencky beam is composed of rigid elements connected by rotational springs (Hencky, 1920), which asymptotically converges towards Euler beam at the continuum limit.

Even if Hencky introduced his model one century ago as a numerical method based on physical arguments to approximate the buckling loads of elastic Euler columns, the treatment of the geometrically exact Hencky problem is more recent and dates from the 80's (with contributions of El Naschie et al, 1988; Gáspár and Domokos, 1989 or Domokos, 1993). El Naschie et al, 1988 numerically computed the curvature of the primary bifurcated branches of the geometrically exact Hencky system, from an asymptotic procedure. Gáspár and Domokos, 1989 or Domokos, 1993 highlighted the very rich structure of the bifurcation diagram of Hencky system with a very exhaustive portrait. Challamel et al (2015-a) decomposed the nonlinear eigenvalue problem of the nonlinear Hencky system into a set of difference equations, and analytically confirmed the curvature values computed by El Naschie et al (1988) for Hencky system. In the present paper, we will apply the same mathematical approach for a nonlinear difference eigenvalue problem which is similar (even if not equivalent) to the geometrically exact Hencky column.

We will show that exact analytical solutions of the post-buckling branches are also available for the granular problem with few numbers of grains. The granular column asymptotically behaves as an Engesser-Timoshenko column (or continuous Cosserat beam model) for a sufficient large number of grains.

2. The granular model – Geometrically exact framework

The *granular elastica* model is a discrete column composed of n+1 rigid discs of radius R and diameter a=2R. In the initial configuration the discs are in contact and their centers lie in a vertical line, which is aligned with axis x of the coordinate frame. The horizontal (lateral) displacement of the center of disc i is denoted by w_i. The rotation of disc i is denoted by θ_i. The axis of the granular elastica (column axis) is the polygon connecting the disc centres, with $\psi_{i+1/2}$ being the angle of the polygon segment between discs i and i+1 from axis x:

$$\psi_{i+1/2} = \arcsin \frac{w_{i+1} - w_i}{a} \tag{1}$$

Figure 1 shows a schematic of the model. It is assumed that the discs cannot separate, i.e. neighbouring discs are always in contact, and the friction coefficient is zero. The interactions between the grains are maintained by bending and shear springs. The bending springs are linear rotational springs connecting each pair of neighbouring discs. The moment arising in rotational spring i is proportional to $\theta_{i+1} - \theta_i$ and the constant of proportionality is $C_R=EI/a$, the discrete bending stiffness.

The shear springs are linear rotation springs connecting each disc to the column axis. Hence disc i is connected to both column axis segments above and below by separate shear springs. The discrete shear strain is defined as

$$\gamma_{i+1/2} = \psi_{i+1/2} - \frac{\theta_i + \theta_{i+1}}{2} \tag{2}$$

Note that it follows Engesser's shear strain theory: the shear strain is the slope of the column axis minus the slope of the bending line, which is computed as the average rotation of the corresponding discs, $(\theta_i + \theta_{i+1})/2$. The discrete shear stiffness is κGAa, the sum of stiffness of shear springs attached to a segment of the column axis. The initial configuration for the springs is stress free. A schematic of two neighbouring discs after deformation is shown in Figure 2. It is worth mentioning that there is an equivalence between the modeling of the granular chain using a classical DEM model based on rotational and shear slip interactions (with stiffness $C_R=EI/a$ and $k_t = \kappa GA/a$), as considered for instance by Serrano and Rodriguez-Ortiz (1973), Cundall and Strack (1979) or more recently Hunt et al, (2010) if the normal interaction is neglected, and the present model based on rotational bending and shear interactions (see Figure 3).

The *granular elastica* equations may be obtained from the following energy function in a geometrically nonlinear exact framework:

$$\frac{\pi}{a} = \frac{1}{2}\sum_{i=0}^{n-1} EI\left(\frac{\theta_{i+1} - \theta_i}{a}\right)^2 + \frac{1}{2}\sum_{i=0}^{n-1} \kappa GA\left(\psi_{i+1/2} - \frac{\theta_i + \theta_{i+1}}{2}\right)^2 - \sum_{i=0}^{n-1} P\left[1 - \cos\left(\psi_{i+1/2}\right)\right] \tag{3}$$

which is consistent with the energy equation considered by Hunt et al (2010) for a *granular elastica* on elastic foundation.

The angle $\psi_{i+1/2}$ can be also reformulated from the discrete displacement variables as:

$$\cos\psi_{i+1/2} = \sqrt{1-\left(\frac{w_{i+1}-w_i}{a}\right)^2} \tag{4}$$

Eq. (3) is a discrete form of the continuous Engesser elastica formulation:

$$\pi = \int_0^L \frac{1}{2}EI\theta'^2 + \frac{1}{2}\kappa GA(\psi-\theta)^2 - P(1-\cos\psi)\,dx \tag{5}$$

From stationarity of the discrete total potential energy given by Eq. (3), $\delta\pi = 0$, the coupled nonlinear difference equations are obtained for the granular *elastica*:

$$\begin{cases} EI\dfrac{\theta_{i+1}-2\theta_i+\theta_{i-1}}{a^2} + \kappa GA\left(\dfrac{\psi_{i+1/2}+\psi_{i-1/2}}{2} - \dfrac{\theta_{i+1}+2\theta_i+\theta_{i-1}}{4}\right) = 0 \\ \kappa GA\left(\psi_{i+1/2} - \dfrac{\theta_i+\theta_{i+1}}{2}\right) - P\sin\psi_{i+1/2} = 0 \end{cases} \tag{6}$$

which again is a discrete form of the differential equations obtained from the continuous total potential energy Eq. (5):

$$\begin{cases} EI\theta'' + \kappa GA(\psi-\theta) = 0 \\ \kappa GA(\psi-\theta) - P\sin\psi = 0 \end{cases} \tag{7}$$

For the shear continuous problem, from Eq. (7), it is possible to express θ as a function of ψ:

$$\theta = \psi - \frac{P}{\kappa GA}\sin\psi \tag{8}$$

The continuous Engesser elastica problem can be reduced to a single nonlinear differential equation already derived by Atanackovic (1997) or Kocsis et al (2017):

$$EI\left[\psi - \frac{P}{\kappa GA}\sin\psi\right]'' + P\sin\psi = 0 \tag{9}$$

The difference equations of the *granular elastica* problem may be also rewritten from Eq. (6), as:

$$\begin{cases} EI\,\dfrac{\theta_{i+1} - 2\theta_i + \theta_{i-1}}{a^2} + \kappa GA\left(\dfrac{\psi_{i+1/2} + \psi_{i-1/2}}{2} - \dfrac{\theta_{i+1} + 2\theta_i + \theta_{i-1}}{4}\right) = 0 \\ EI\,\dfrac{\theta_{i+1} - 2\theta_i + \theta_{i-1}}{a^2} + P\left(\dfrac{\sin\psi_{i+1/2} + \sin\psi_{i-1/2}}{2}\right) = 0 \end{cases} \tag{10}$$

It could be convenient to introduce the difference operators:

$$\delta_0 w_i = \frac{w_{i+1} + 2w_i + w_{i-1}}{4} \quad , \; \delta_1 w_i = \frac{w_{i+1} - w_{i-1}}{2a} \quad \text{and} \quad \delta_2 w_i = \frac{w_{i+1} - 2w_i + w_{i-1}}{a^2} \tag{11}$$

It is also possible to express these last difference operators with respect to the shift operator $\boldsymbol{E}$ (see Goldberg, 1958; Elaydi, 2005):

$$\delta_0 = \frac{1}{4}\left(\boldsymbol{E} + 2\boldsymbol{I} + \boldsymbol{E}^{-1}\right), \; \delta_1 = \frac{1}{2a}\left(\boldsymbol{E} - \boldsymbol{E}^{-1}\right) \text{ and } \quad \delta_2 = \frac{1}{a^2}\left(\boldsymbol{E} - 2\boldsymbol{I} + \boldsymbol{E}^{-1}\right) \tag{12}$$

where $\boldsymbol{I}$ is the identity operator. It is easy to check the remarkable property:

$$\delta_0\delta_2 = \delta_2\delta_0 = \delta_1^2 \tag{13}$$

It is also possible to introduce the related difference operator:

$$\sqrt{\delta_0}\, w_i = \frac{w_{i+1/2} + w_{i-1/2}}{2} \qquad \text{with} \;\; \sqrt{\delta_0}\, w_i = \delta_0^{1/2} w_i = \frac{1}{2}\left(\boldsymbol{E}^{1/2} + \boldsymbol{E}^{-1/2}\right) w_i \tag{14}$$

The nonlinear granular elastica problem Eq. (10) is then reformulated with these difference operators as:

$$\begin{cases} EI\delta_2\theta_i + \kappa GA\left(\sqrt{\delta_0}\psi_i - \delta_0\theta_i\right) = 0 \\ EI\delta_2\theta_i + P\sqrt{\delta_0}\sin\psi_i = 0 \end{cases} \tag{15}$$

which makes possible to extract θ_i from the first nonlinear difference equation Eq. (15), as :

$$\delta_0\theta_i = \sqrt{\delta_0}\psi_i - \frac{P}{\kappa GA}\sqrt{\delta_0}\sin\psi_i \tag{16}$$

It is possible to apply the difference operator δ_0 to the second equation of Eq. (15) thus leading to:

$$EI\delta_2\delta_0\theta_i + P\delta_0\sqrt{\delta_0}\sin\psi_i = 0 \tag{17}$$

The consideration of both Eq. (16) and Eq. (17) finally gives the single nonlinear difference equation:

$$EI\delta_2\sqrt{\delta_0}\left(\psi_i - \frac{P}{\kappa GA}\sin\psi_i\right) + P\delta_0\sqrt{\delta_0}\sin\psi_i = 0 \tag{18}$$

which can be reformulated by difference integration:

$$EI\delta_2\left(\psi_i - \frac{P}{\kappa GA}\sin\psi_i\right) + P\delta_0\sin\psi_i = 0 \tag{19}$$

The granular elastica problem can then be obtained equivalently from a single nonlinear difference equation Eq. (19) or equivalently:

$$EI\frac{\psi_{i+1} - 2\psi_i + \psi_{i-1}}{a^2} - P\frac{EI}{\kappa GA}\frac{\sin\psi_{i+1} - 2\sin\psi_i + \sin\psi_{i-1}}{a^2} + P\frac{\sin\psi_{i+1} + 2\sin\psi_i + \sin\psi_{i-1}}{4} = 0 \tag{20}$$

which is a finite difference scheme of the continuous granular elastica, in fact equivalent to the Engesser elastica problem governed by the nonlinear differential equation Eq. (9).

The granular elastica differs from the discrete Engesser elastica explored in Kocsis et al (2017):

$$\begin{cases} EI\dfrac{\theta_{i+1}-2\theta_i+\theta_{i-1}}{a^2}+\kappa GA\left(\psi_i-\theta_i\right)=0 \\ EI\dfrac{\theta_{i+1}-2\theta_i+\theta_{i-1}}{a^2}+P\sin\psi_i=0 \end{cases} \tag{21}$$

In fact, for the discrete Engesser elastica problem defined by Eq. (21) and investigated in Kocsis et al (2017), it is possible to express one variable with respect to the other:

$$\theta_i=\psi_i-\frac{P}{\kappa GA}\sin\psi_i \tag{22}$$

From the discrete Engesser elastica explored in Kocsis et al (2017), it is then possible to derive a single second-order nonlinear difference equation by using both Eq. (21) and Eq. (22):

$$EI\frac{\psi_{i+1}-2\psi_i+\psi_{i-1}}{a^2}-P\frac{EI}{\kappa GA}\frac{\sin\psi_{i+1}-2\sin\psi_i+\sin\psi_{i-1}}{a^2}+P\sin\psi_i=0 \tag{23}$$

Comparing Eqs. (20) and (23) clearly shows the differences between the discrete granular elastica and the discrete Engesser elastica considered by Kocsis et al (2017). Both discrete systems converge towards the continuous Engesser elastica but from two distinguished discrete schemes.

Note that the difference equations explored for the granular elastica also differs from the shear difference equations of Kocsis (2016) who explored a discrete Haringx-type model.

By introducing the following dimensionless parameters,

$$\beta = \frac{PL^2}{EI} \text{ and } s^2 = \frac{EI}{\kappa GAL^2} \tag{24}$$

The dimensionless *granular elastica* problem can be expressed from the coupled system of nonlinear difference equations:

$$\begin{cases} \theta_{i+1} - 2\theta_i + \theta_{i-1} + \dfrac{1}{s^2 n^2}\left(\dfrac{\psi_{i+1/2} + \psi_{i-1/2}}{2} - \dfrac{\theta_{i+1} + 2\theta_i + \theta_{i-1}}{4} \right) = 0 \\ \theta_{i+1} - 2\theta_i + \theta_{i-1} + \dfrac{\beta}{n^2}\left(\dfrac{\sin\psi_{i+1/2} + \sin\psi_{i-1/2}}{2} \right) = 0 \end{cases} \tag{25}$$

Eq. (25) can be equivalently reformulated with the discrete displacement field as:

$$\begin{cases} \theta_{i+1} - 2\theta_i + \theta_{i-1} + \dfrac{1}{s^2 n^2}\left[\dfrac{\arcsin\left(\dfrac{w_{i+1} - w_i}{a} \right) + \arcsin\left(\dfrac{w_i - w_{i-1}}{a} \right)}{2} - \dfrac{\theta_{i+1} + 2\theta_i + \theta_{i-1}}{4} \right] = 0 \\ \theta_{i+1} - 2\theta_i + \theta_{i-1} + \dfrac{\beta}{n^2}\left(\dfrac{w_{i+1} - w_{i-1}}{2a} \right) = 0 \end{cases} \tag{26}$$

The nonlinear boundary value problem of the granular *elastica* is then governed by Eq. (25) coupled to the symmetrical boundary conditions for the simply supported granular column:

$$\theta_1 = \theta_{-1},\ \psi_{1/2} = \psi_{-1/2}\ ,\ \theta_{n-1} = \theta_{n+1} \text{ and } \psi_{n-1/2} = \psi_{n+1/2} \tag{27}$$

The granular elastica may be also investigated from the equivalent single dimensionless nonlinear difference equation:

$$a^2\delta_2\left(\psi_i-\beta s^2\sin\psi_i\right)+\frac{\beta}{n^2}\delta_0\sin\psi_i=0 \tag{28}$$

or equivalently:

$$\psi_{i+1}-2\psi_i+\psi_{i-1}-\beta s^2\left(\sin\psi_{i+1}-2\sin\psi_i+\sin\psi_{i-1}\right)+\frac{\beta}{4n^2}\left(\sin\psi_{i+1}+2\sin\psi_i+\sin\psi_{i-1}\right)=0 \tag{29}$$

3. The granular model – Linear analysis

The calculation of the buckling load of the granular elastica may be achieved by linearization of the nonlinear difference eigenvalue problem. The linearization of the coupled system of difference equations Eq. (6) is expressed by:

$$\begin{cases} EI\dfrac{\theta_{i+1}-2\theta_i+\theta_{i-1}}{a^2}+\kappa GA\left(\dfrac{\psi_{i+1/2}+\psi_{i-1/2}}{2}-\dfrac{\theta_{i+1}+2\theta_i+\theta_{i-1}}{4}\right)=0 \\ \left(P-\kappa GA\right)\psi_i+\kappa GA\dfrac{\theta_{i-1/2}+\theta_{i+1/2}}{2}=0 \end{cases} \tag{30}$$

This linear system of difference equations, expressed with the shear-rotation variables may be easily reformulated in a rotation-displacement discrete space, using the linearized kinematic constraint:

$$\psi_i=\sqrt{\delta_2}w_i=\frac{w_{i+1/2}-w_{i-1/2}}{a} \tag{31}$$

Considering now the second equation of Eq. (30), equivalently leads, thanks to the remarkable property Eq. (13), to:

$$\left(P-\kappa GA\right)\sqrt{\delta_2}w_i+\kappa GA\sqrt{\delta_0}\theta_i=0 \quad\Rightarrow\quad \left(P-\kappa GA\right)\delta_2 w_i+\kappa GA\,\delta_1\theta_i=0 \tag{32}$$

The linearized difference equations are then expressed with the rotation and displacement discrete fields, given below:

$$\begin{cases} EI\dfrac{\theta_{i+1}-2\theta_i+\theta_{i-1}}{a^2}+\kappa GA\left(\dfrac{w_{i+1}-w_{i-1}}{2a}-\dfrac{\theta_{i+1}+2\theta_i+\theta_{i-1}}{4}\right)=0 \\ \left(P-\kappa GA\right)\dfrac{w_{i+1}-2w_i+w_{i-1}}{a^2}+\kappa GA\dfrac{\theta_{i+1}-\theta_{i-1}}{2a}=0 \end{cases} \tag{33}$$

This coupled system of difference equations, already derived by Challamel et al (2020) from a linearization process in the energy equation, can be alternatively written in a matrix format, of difference operators:

$$\begin{pmatrix} EI\delta_2-\kappa GA\delta_0 & \kappa GA\delta_1 \\ \kappa GA\delta_1 & \left(P-\kappa GA\right)\delta_2 \end{pmatrix}\begin{pmatrix} \theta_i \\ w_i \end{pmatrix}=\begin{pmatrix} 0 \\ 0 \end{pmatrix} \tag{34}$$

Calculating the determinant of the matrix of difference operators in Eq. (34) and using the remarkable property Eq. (13) gives the final linear fourth-order difference equation for the deflection:

$$EI\left(1-\frac{P}{\kappa GA}\right)\delta_2^2 w_i+P\delta_2\delta_0 w_i=0 \tag{35}$$

Eq. (35) is a finite difference scheme for the buckling problem of the Engesser-Timoshenko continuous column.

Eq. (35) can be integrated (in the sense of difference method) twice:

$$EI\left(1-\frac{P}{\kappa GA}\right)\delta_2 w_i+P\delta_0 w_i=P\left(A+Bi\right) \tag{36}$$

where $\left(A,B\right)$ are two constants of integration. This linear difference equation can be solved by assuming a displacement solution in a form of power function for the second-order difference equation without second member (Goldberg, 1958):

$$w_i = w_0 \lambda^i \tag{37}$$

The substitution of Eq. (37) into the difference equation Eq. (36) without second member, furnishes the following auxiliary equation:

$$\left(1-\beta s^2+\frac{\beta}{4n^2}\right)\lambda^2-2\left(1-\beta s^2-\frac{\beta}{4n^2}\right)\lambda+1-\beta s^2+\frac{\beta}{4n^2}=0 \tag{38}$$

The auxiliary equation admits two complex conjugate solutions

$$\lambda = 1-\frac{\frac{\beta}{2n^2}}{1-\beta s^2+\frac{\beta}{4n^2}} \pm \sqrt{\left(1-\frac{\frac{\beta}{2n^2}}{1-\beta s^2+\frac{\beta}{4n^2}}\right)^2-1} = \cos\varphi \pm j\sin\varphi \qquad \text{with}$$

$$\cos\varphi = 1-\frac{\frac{\beta}{2n^2}}{1-\beta s^2+\frac{\beta}{4n^2}} \quad \text{and} \quad j^2=-1 \tag{39}$$

The general solution for the linear difference equation Eq. (36) can finally be expressed in polynomial and trigonometric functions:

$$w_i = A + iB + C\cos(\varphi i) + D\sin(\varphi i) \tag{40}$$

Now considering the four boundary conditions Eq. (27) of the hinge-hinge granular column reformulated in terms of displacement

$$w_0 = 0\,,\ w_1 = -w_{-1} \quad ,\ w_n = 0 \ \text{ and } \ w_{n+1} = -w_{n-1} \tag{41}$$

gives:

$$A = B = C = 0 \qquad \text{and} \qquad \sin(n\varphi) = 0 \tag{42}$$

With the constants $A = B = 0$ vanishing, the second member of Eq. (36) is vanishing:

$$EI\left(1-\frac{P}{\kappa GA}\right)\delta_2 w_i + P\delta_0 w_i = 0 \tag{43}$$

For simply supported boundary conditions, the linearized problem can be obtained from the second-order linear difference equation Eq. (43):

$$\left(1-\frac{P}{\kappa GA}\right)EI\,\frac{w_{i+1}-2w_i+w_{i-1}}{a^2} + P\,\frac{w_{i+1}+2w_i+w_{i-1}}{4} = 0 \tag{44}$$

This model is in fact similar to the model of Kocsis (2016), in case of shear inextensible elements (discrete Euler-Bernoulli beam element; $\kappa GA \to \infty$):

$$EI\,\frac{w_{i+1}-2w_i+w_{i-1}}{a^2} + P\,\frac{w_{i+1}+2w_i+w_{i-1}}{4} = 0 \tag{45}$$

This second-order linear difference equation Eq. (45) is also the one reported by Satake (1998) for the buckling of a granular column in the absence of shear interaction (see Eq. (7) of the paper of Satake, 1998)). In other words, Eq. (44) of the present paper generalizes the results of Satake (1998) for both rotational and shear granular interactions.

For the granular column studied in this paper, considering Eq. (42) gives for the fundamental buckling mode of trigonometric form (as assumed by Challamel et al, 2020 in presence of additional discrete soil elastic interactions):

$$\varphi = \frac{\pi}{n} \quad \Rightarrow \quad w_i = D\sin\left(\pi\frac{i}{n}\right) \tag{46}$$

Furthermore, the buckling load is expressed as:

$$\cos\frac{\pi}{n} = 1-\frac{\dfrac{\beta}{2n^2}}{1-\beta s^2+\dfrac{\beta}{4n^2}} \quad \Rightarrow \quad \beta = \frac{4n^2\sin^2\left(\dfrac{\pi}{2n}\right)}{\cos^2\left(\dfrac{\pi}{2n}\right)+4s^2n^2\sin^2\left(\dfrac{\pi}{2n}\right)} \tag{47}$$

which has been obtained by Challamel et al (2020) in presence of additional Winkler and Pasternak-type foundation.

Engesser formulae, valid for the buckling of columns in presence of shear effects (Engesser, 1891 – see also Timoshenko and Gere, 1961) is asymptotically found in the continuum limit:

$$\lim_{n\to\infty} \beta = \frac{\pi^2}{1+\pi^2 s^2} = \frac{\beta_E}{1+\beta_E s^2} \quad \text{with} \quad \beta_E = \pi^2 \tag{48}$$

The granular column then asymptotically behaves as an Engesser-Timoshenko column, in the continuum limit.

From Eq. (48), the pure granular system with only bending interactions *s=0* has a buckling load equal to:

$$s = 0 \quad \Rightarrow \quad \beta = 4n^2 \tan^2\left(\frac{\pi}{2n}\right) \tag{49}$$

which has been also obtained by Kocsis (2016) for a hinge-hinge Cosserat chain.

Figure 4 shows the (fundamental) buckling load parameter as function of *n* for various stiffness parameter values *s* based on Eq (47).

Alternative boundary conditions may be considered as well, as investigated by Satake (1998) (see also the calculation in Appendix A).

4. Analytical solutions for few grains

For the case of two grains only the trivial equilibrium state exists. It can be seen from the equations, but also intuitively as both grains are constrained against lateral displacement by the supports and the point of action of the force cannot be displaced.

For the granular column of a few grains some analytical solutions can be developed. For the derivations we will make use of the geometric constraint

$$\sum_{i=0}^{n-1} \sin \psi_{i+1/2} = 0 \tag{50}$$

The above equality can be obtained from the summation of the second set of equations of Eq. (25), assuming non-zero loading, and means that the centres of the first and the last grains lie on a vertical line.

4.1 A three-grain granular column

For three grains (n=2) it is possible to find all the solutions for the system of nonlinear equations Eq. (25) analytically.

Eq (50) in this case yields:

$$\sin \psi_{1/2} + \sin \psi_{1+1/2} = 0 \tag{51}$$

Eq. (51) holds for any $\psi_{1/2}$ if one of the following equalities is fulfilled:

$$\begin{aligned} \psi_{1+1/2} &= -\psi_{1/2} - 2k\pi \\ \psi_{1+1/2} &= \psi_{1/2} - (2m+1)\pi \end{aligned} \tag{52}$$

Here k and m are integers. Hence two families of equilibrium paths for three grains can be found:

$$\begin{aligned} \beta &= \frac{4n^2}{1+4s^2n^2} \frac{\psi_{1/2} + k\pi}{\sin \psi_{1/2}} \\ \beta &= \frac{2n^2}{1+4s^2n^2} \frac{(2m+1)\pi}{\sin \psi_{1/2}} \end{aligned} \tag{53}$$

The derivation for Eq. (53) is given in Appendix B.

4.2 A four-grain granular column

For the granular elastica of four grains (n=3) it is possible to analytically find equilibrium configurations that obeys some symmetries, but not all the solutions in general.

The geometric constraint Eq. (50) for four grains is:

$$\sin\psi_{1/2} + \sin\psi_{1+1/2} + \sin\psi_{2+1/2} = 0 \tag{54}$$

A solution for Eq. (54) assumes reflection symmetry to the vertical axis:

$$\begin{aligned} \psi_{2+1/2} &= -\psi_{1/2} - 2k\pi \\ \psi_{1+1/2} &= m\pi \end{aligned} \tag{55}$$

Here k and m are integers. Following a similar approach as in Appendix B, we can obtain the analytical solutions for mirror-symmetric configurations using geometrically exact description:

$$\beta = \frac{4n^2}{3+4s^2n^2}\frac{\psi_{1/2}+k\pi}{\sin\psi_{1/2}} \tag{56}$$

Another set of solutions for Eq. (54) obeys point symmetry:

$$\begin{aligned} \psi_{2+1/2} &= \psi_{1/2} + 2k\pi \\ \sin(\psi_{1+1/2}) &= -2\sin(\psi_{1/2}) \end{aligned} \tag{57}$$

Here k is integer. The analytical solution with point-symmetric equilibrium configurations using geometrically exact description is:

$$\beta = \frac{4n^2}{1+12s^2n^2}\frac{f(\psi_{1/2})}{\sin\psi_{1/2}} \tag{58}$$

where

$$f(\psi_{1/2}) = \begin{cases} \psi_{1/2} + \arcsin(2\sin(\psi_{1/2})) + 2k\pi \\ \psi_{1/2} - \arcsin(2\sin(\psi_{1/2})) + (2k+1)\pi \end{cases} \quad \begin{matrix} if \quad \mathrm{mod}(|\psi_{1+1/2}|, 2\pi) < \dfrac{\pi}{2} \\ else \end{matrix} \qquad (59)$$

and $\sin(\psi_{1/2}) \leq 0.5$.

Derivation of these analytical results is given in Appendix C.

4.3 Approximation of the first post-buckling path for arbitrary number of grains

The analytical solution for the geometrically exact granular elastica of *n* grains can be *approximated* by generalizing the above solutions for mirror-symmetric configurations. The first post-buckling path can be estimated analytically as a possible generalization of the primary post-bifurcation branch in the case *n=2*, as:

$$\frac{\beta}{\beta_0} \approx \frac{\psi_{1/2}}{\sin\psi_{1/2}} \text{ with } \beta_0 = \frac{4n^2 \sin^2\left(\dfrac{\pi}{2n}\right)}{\cos^2\left(\dfrac{\pi}{2n}\right) + 4s^2 n^2 \sin^2\left(\dfrac{\pi}{2n}\right)} \qquad (60)$$

This formulae has not been built from asymptotic arguments and is assumed as a possible approximation of the exact discrete granular problem. This formulae for the primary bifurcation branch is only exact for the specific case *n=2*. Note that the fundamental buckling load Eq (47) can be also obtained with the above formula. Another approximated formulae may be derived from asymptotic arguments, for *n* larger than *3*, as shown in Appendix D.

$$\frac{\beta}{\beta_0} \approx 1 + \frac{\psi_{1/2}^2}{8\cos^2\left(\dfrac{\pi}{2n}\right)} \text{ with } \beta_0 = \frac{4n^2 \sin^2\left(\dfrac{\pi}{2n}\right)}{\cos^2\left(\dfrac{\pi}{2n}\right) + 4s^2 n^2 \sin^2\left(\dfrac{\pi}{2n}\right)} \qquad (61)$$

Eq. (47) can be also obtained, as a limiting case when $\psi_{1/2}$ tends towards zero, from Eq. (61). Eq. (61) is obtained from an asymptotic expansion of both the load and the unknown discrete field with respect to a small parameter, such as the boundary rotation. The method consists in approaching the nonlinear difference eigenvalue problem by a set of linear difference eigenvalue problems which can be analytically solved. Such mathematical approach has been shown to be very efficient for evaluating the post-bifurcation response of Hencky column (Challamel et al, 2015-a). It is shown also in this paper that this asymptotic method is particularly accurate for computing the post-bifurcation branches of the granular *elastica* problem. For *n=2*, the exact equation is given by Eq. (60). For *n=3*, Eq. (60) and Eq. (61) coincide for the sensitivity of the primary bifurcation branch with respect to the square of $\psi_{1/2}$. For *n* larger than *4*, Eq. (61) should be more precise, at least in the vicinity of the bifurcation load, as it is rigorously obtained from an asymptotic expansion.

5. Numerical solutions

5.1 The solution strategy

For the numerical solutions of Eq. (25) with boundary conditions Eq. (27) the governing differential equation systems are further manipulated to eliminate the unknowns $\psi_{i+1/2}$. First $\psi_{i+1/2}$ is expressed from the first equation of Eq. (25) and boundary condition $\psi_{1/2} = \psi_{-1/2}$ is considered, yielding

$$\psi_{i+1/2} = 2s^2 n^2 \left((-1)^i (-\theta_1 + \theta_0) + \sum_{j=1}^{i} (-1)^{i-j} (-\theta_{j+1} + 2\theta_j - \theta_{j-1}) \right) + \frac{\theta_{i+1} + \theta_i}{2} \qquad (62)$$

The derivation of Eq. (62) is given in Appendix E.

Eq. (62) can be substituted in the second equation of Eq. (25), leading to *n*+1 highly nonlinear equation system with *n*+1 unknown rotations $(\theta_0, \theta_1, \cdots, \theta_n)$ and two parameters, s and β. If we fix the stiffness parameter *s*, then the solutions form equilibrium paths uniquely embedded

in an n+2 dimensional space. The space $(\theta_0, \theta_1, \cdots, \theta_n, \beta)$ is called the Global Representation Space (GRS) hereafter.

In our numerical solution strategy, we first implement the simplex algorithm (Domokos and Gáspár, 1995, Gáspár et al, 1997). The algorithm is able to approximate all the solutions of a nonlinear algebraic equation system without iterations in a given bounded domain of the GRS. For doing so it divides the GRS into simplices and solves a linearised equation system over each simplex. The drawback of the algorithm, however, is that the computation requirement increases exponentially with the dimension of the GRS. Therefore, the numerical simulations are computed only for small values of n. The algorithm is coded in FORTRAN 90.

Not only the global solutions can be obtained with the algorithm, but also equilibrium paths can be followed. This is referred to as path following hereafter, which is not limited by the dimension of the GRS as heavily as the scanning.

We have developed a hybrid approach for the numerical simulation. First scanning is implemented with a fairly coarse resolution of the GRS. The obtained results then can be smoothened by the Newton-Raphson method, also coded in FORTRAN 90. The equilibrium branches that we obtain this way are the ones which are inside the scanned, bounded domain. Often the paths seem to be discontinuous as they may exit the scanned domain at some point and may return at another point of the path, or may not return to the scanned domain. Some small parts of the paths can also be missing because of the coarse resolution of the symplectic grid.

To overcome these difficulties the following algorithm is applied as final step. We choose m solutions from what we have already found. Then we apply the path following algorithm starting at these solution points in all possible 2^{n+1} directions. The m solutions are chosen randomly and all the input files for the path following (for all the chosen solution points and for all possible directions) are generated and run automatically, and all the obtained results are merged automatically. This final step is implemented in Python 3. Note that a different hybrid parallel approach of the simplex algorithm is described in (Domokos and Szeberényi, 2004).

Before choosing the domain for scanning, we investigate if certain symmetries can be observed in Eq. (25). Suppose we have an equilibrium state given by the stiffness parameter *s*, the load parameter β and the rotations $(\theta_0, \theta_1, \cdots, \theta_n)$, $(\psi_{1/2}, \psi_{1+1/2}, \cdots, \psi_{n-1/2})$. We obtain another equilibrium configurations if we keep the stiffness parameter *s* unchanged and either:

- Change sign of all the rotations and keep the load unchanged
- Add $k\pi$ to all the rotations and multiply the load by $(-1)^k$

These properties will be taken into account, i.e. we will only scan for positive load β and $\theta_0 \in [0, \pi]$. We do not explore some non-interpenetration conditions in the bifurcation diagram.

5.2 Results

First, we verify the numerical solutions by comparing them to the analytical results. The equilibrium paths obtained numerically are projected on the subspace $\psi_{1/2}, \beta$ and this projections (bifurcation diagrams) are plotted. The rotation $\psi_{1/2}$ can be computed from the scanning result for the grain rotations as:

$$\psi_{1/2} = 2s^2 n^2 (-\theta_1 + \theta_0) + \frac{\theta_1 + \theta_0}{2} \tag{63}$$

For the derivation of Eq. (63), see Appendix E.

Figure 5 shows all the solutions of the nonlinear equation system found numerically for *n*=2 (three grains) and *s*=0.1, 0.3, 0.4, 0.5, 0.6, 0.7, and 1.0. The scanning was run on the bounded domain $\theta_0 \in [0, \pi]$, $\theta_1, \theta_2 \in [-2\pi, 2\pi]$ and $\beta \in (0, 30]$. The resolution of the GRS is 150x600x600x400. For validation, the analytical solutions, given by Eq. (53), are also plotted with dashed black lines and by black dots. It can be seen that the solutions found by the numerical procedure and the analytical results are identical which validates the numerical implementation. As detailed in Appendix B and confirmed by the bifurcation diagram of Figure 5, the primary branch is intersected by a secondary branch at point $\left(\psi_{1/2} = \pi/2, \beta = \beta_0\, \pi/2\right)$. This secondary branch is a rigid rotation mechanism (the structure becomes kinematically indeterminate) which corresponds to the superposition of grain 2 with grain 0. It is worth mentioning that the interpenetration condition between rigid grains has not

been included in the model. If a non-interpenetration condition between grain 0 and grain 2 is explicitly considered, an additional kinematics constraint has to be taken into account. These additional constraints need to be incorporated for a fully realistic post-bifurcation granular analysis.

Figure 6 shows all the equilibrium paths of the granular elastica of three grains in the bounded domain of the load parameter $\beta \in [-30,30]$ and $\psi_{1/2} \in [-2\pi,2\pi]$ based on the analytical solutions given by Eq. (53). An animation is provided as electronic supplementary material showing the equilibrium branches with slowly changing stiffness parameter $s \in (0,1.5]$.

Figure 7 shows all the solutions of the nonlinear equation system found numerically for n=3 (four grains) and s=0.4, 0.5, 0.6 and 0.7. The scanning was accomplished on the bounded domain $\theta_0 \in [0,\pi]$, $\theta_1,\theta_2,\theta_3 \in [-2\pi,2\pi]$ and $\beta \in (0,30]$. The resolution of the GRS is 75x300x300x225. For validation the analytical solutions, given by Eq. (56) and (58), are also plotted with dashed black lines. It can be seen that apart from the reflection and point symmetric equilibrium configurations, there are many more solutions found numerically. Even if n=3 is not a large number of grains, it can be observed that instability branches exist for such discrete structural problem, that are not present for the continuous Engesser column. This phenomenon was already highlighted for discrete shear columns by Kocsis et al (2017), or by Kocsis and Challamel (2018) for extensible discrete shear columns. These results are similar to the rich bifurcation diagram observed for the bifurcation diagram of discrete Euler column (modeled by Hencky-Chain model), as shown by Gáspár and Domokos (1989), Domokos (1993), Domokos and Holmes (1993) or Domokos and Holmes (2003) with the so-called additional parasitic solutions.

The computation for n=3 on $\theta_0 \in [0,\pi]$, $\theta_1,\theta_2,\theta_3 \in [-2\pi,2\pi]$ and $\beta \in (0,30]$ with GRS resolution 75x300x300x225 took ~7 days 2 hours 44 minutes on three cores of an Intel(R) Core(TM) 2 Quad Q8200 processor @2.33 GHz. The load parameter domain was split in three parts for the three cores. The output of the scanning was refined with the Newton-Raphson method and the path following for randomly chosen equilibrium configurations were accomplished, following the procedure described in Section 5.1. The last two steps did not need much time, less than 1 hour in total. It can be seen that scanning is far the most expensive part of the simulation in terms of computational resources. That is the reason why

we have developed a hybrid approach that tries to minimize the cost of scanning by using a coarse resolution of the GRS.

Finally, Figure 8 shows the equilibrium paths obtained with the path following algorithm for n=2,3,..,9 with stiffness parameter s=0.4 for $\psi_{1/2} < \pi/4$. The analytical estimate of the first post-buckling path, as given by Eq. (60) and Eq. (61), are also shown. It can be seen that the approximate solution Eq. (60) is better aligned with the numerical results for smaller number of grains, while Eq. (61), obtained from asymptotic expansion, is a better estimate for larger number of grains. Figure 9 shows these paths up to $\psi_{1/2} = \pi$. As the formula Eq. (61) neglects higher order terms, with larger displacements it becomes less accurate. It can be observed in Figure 9 that the first post-buckling path bifurcates for odd number of grains (even n). It may be a general behaviour as a similar phenomenon was already observed for the elastic linkage (Gáspár and Domokos, 1989). It is worth mentioning that the path following algorithm typically follows a bifurcated branch at a bifurcation point. That is why in Figure 9, for odd number of grains, we cannot see the continuation of the first post-buckling path after the bifurcation point, the algorithm followed a secondary branch.

6. Conclusions

This paper investigates the buckling and post-buckling behavior of a granular column. The column is composed of rigid grains elastically connected by translational and rotational links. The mechanical problem is formulated in a geometrically exact framework, in order to capture exactly the various post-bifurcation branches. This discrete mechanics problem is ruled by some nonlinear difference equations. The post-bifurcation branches have been computed using a simplex algorithm, and have been compared to analytical solutions for a few grains (for a chain composed of three grains – case $n=2$, it was possible to express all post-bifurcation branches analytically). To the authors' knowledge, the complete bifurcation diagram of the granular *elastica* was not available in the literature, even for few grains. It is hoped that the results presented in this paper could contribute to a better understanding of the complex instability phenomena in granular materials. Clearly, instability branches exist for such discrete structural problem, that are not present for the continuous Engesser column. This phenomenon was already highlighted for discrete shear columns by Kocsis et al (2017), or by Kocsis and Challamel (2018) for extensible discrete shear columns. These results are similar to the rich bifurcation diagram observed for the geometrically exact bifurcation analysis of Hencky chain under axial force (discrete Euler column), as shown by Gáspár and Domokos (1989), Domokos (1993), Domokos and Holmes (1993) or Domokos and Holmes (2003) with the so-called parasitic solutions. A granular column also belongs to the class of discrete Engesser columns with a bifurcation diagram different from the asymptotic continuous Engesser column due to its inherent discrete nature (this fundamental aspect of the discreteness versus continuous limit is extensively discussed by Domokos and Holmes for Hencky chains).

The idea of investigating the granular column using the method of finite differences is due to Satake (1998) who considered this paradigmatic granular (discrete) column, for a better understanding of the instability patterns in the localization process due to shear band formation in granular media. Satake (1998) only considered the linearized buckling analysis of a particle column in the formation of shear band. The results presented in this paper also show the capability of this paradigmatic system in the nonlinear range. An asymptotic expansion method has been applied to the nonlinear difference eigenvalue problem, to get a

very accurate approximate solution of the primary post-bifurcation branch of the nonlinear granular *elastica* problems. It could be interesting to explore the capability of higher-order continuous medium to capture the scale effect of this granular column, as explored for Hencky-type model in the nonlinear range by Challamel et al (2015-a) or Challamel et al (2015-b) without shear interaction, and by Kocsis et al (2017) or Kocsis and Challamel (2018) in presence of shear and rotational discrete interactions. In such localized zone, some two-dimensional features may be predominant. The present study also explores the nonlinear domain with an exhaustive representation of the post-bifurcation branches. The geometrically exact analysis of two-dimensional granular instabilities (also including the coupling with the normal stiffness of the granular interaction) is a much more complex problem, which could be investigated in the future, for a better understanding of generic instabilities in geomechanics.

Acknowledgements

The authors would like to thank Prof. Félix Darve, Prof. Jean Lerbet, Prof. François Nicot and Dr. Antoine Wautier for fuitful discussions on granular models.

6. References:

Andreotti B., Forterre Y. and Pouliquen O., *Granular media – Between fluid and solid*, Cambridge University Press, Cambridge, 2013.

Atanackovic T.M., *Stability theory of elastic rods*, Series on Stability, Vibration and Control of Systems, Series A: Volume 1, World Scientific, Singapore, 1997.

Battista A., Della Corte A., dell'Isola F. and Seppecher P., Large deformations of 1d microstructured systems modeled as generalized Timoshenko beams, *Z. Angew. Math. Phys.* 69, 3, 52, 2018.

Boscovich R.J., *Theoria philosophiae naturalis*, 1st ed., Venice, 1763**,** English edition with a short life of Boscovich, Chicago and London, 1922**.**

Cambou B., Jean M. and Radjai F. (Eds), *Micromechanics of granular materials*, ISTE-Wiley, London, 2009.

Capecchi D., Ruta G. and Trovalusci P., From classical to Voigt's molecular models in elasticity, *Arch. Hist. Exact Sciences*, 64, 525-559, 2010.

Cauchy A., Sur l'équilibre et le mouvement d'un système de points matériels sollicités par des forces d'attraction ou de répulsion mutuelle, *Exercices de Mathématiques* 3:188–212, 1828 (in French).

Challamel N., Lerbet J. and Wang C.M., On buckling of granular columns with shear interaction: discrete versus nonlocal approaches, *J. Applied Physics*, 115, 234902, 2014.

Challamel N., Kocsis A. and Wang C.M., Discrete and nonlocal *elastica*, *Int. J. Non-linear Mech.*, 77, 128-140, 2015-a.

Challamel N., Kocsis A. and Wang C.M., Higher-order gradient elasticity models applied to geometrically nonlinear discrete systems, *Theoretical and Applied Mechanics*, 42, 4, 223-248, 2015-b.

Challamel N., Lerbet J., Darve F. and Nicot F., Buckling of granular systems with discrete and gradient elasticity Cosserat continua, *Annals of Solid Structural Mechanics*, 12, 7-22, 2020.

Cundall P.A., A computer model for simulating progressive, large-scale movements in blocky rock systems, *Proc. Symp. Int. Sot. Rock Mech.*, Nancy, 1, 132-150, 1971.

Cundall P.A. and Strack O.D.L., A discrete numerical model for granular assemblies, *Geotechnique*, 29, 1, 47–65, 1979.

Dell'Isola F. and Steigmann D.J. (Eds), *Discrete and continuum models for complex metamaterials*, Cambridge University Press, 2020.

Domokos G., Qualitative convergence in the discrete approximation of the Euler problem, *Mech. Struct. Mach.*, 21, 4, 529–43, 1993.

Domokos G., Gáspár Zs., A global, direct algorithm for path-following and active static control of elastic bar structures, *Mechanics of Structures and Machines* 23:549–571, 1995.

Domokos G. and Holmes P., Euler's problem and Euler's method, or the discrete charm of buckling, *J. Nonlinear Sci.*, 3, 109–151, 1993.

Domokos G. and Holmes P., On nonlinear boundary-value problems: ghosts, parasites and discretizations, *Proc. Royal Soc. London* A, 459, 1535–1561, 2003.

Domokos G. and Szeberényi I., A hybrid parallel approach to one-parameter nonlinear boundary value problems, *Computer Assisted Mechanics and Engineering Sciences*, 11:15–34, 2004.

El Naschie M.S., Wu C.W. and Wifi A.S., A simple discrete element method for the initial postbuckling of elastic structures, *Int. J. Num. Meth. Eng.*, 26, 2049-2060, 1988.

Engesser F., Die Knickfestigkeit gerader Stäbe, *Zentralblatt der Bauverwaltung*, 11, 483-486, 1891.

Gáspár Z. and Domokos G., Global investigation of discrete models of the Euler buckling problem, *Acta Technica Acad. Sci. Hung.*, 102, 227-238, 1989.

Gáspár Zs., Domokos G., and Szeberényi I., A parallel algorithm for the global computation of elastic bar structures, *CAMES*, 4:55–68, 1997.

Hencky H., Über die angenäherte Lösung von Stabilitätsproblemen im Raummittels der elastischen Gelenkkette, *Der Eisenbau*, 11, 437-452, 1920 (in German).

Hunt G.W., Tordesillas A., Green S.C. and Shi J., Force-chain buckling in granular media: a structural mechanics perspective, *Phil. Trans. R. Soc. A*, ,368, 1910, 249-262, 2010.

Hutter K. and Wilmanski K., *Kinetic and continuum theories of granular and porous media*, CISM n°400, Springer, Springer-Verlag, 1999.

Károlyi G. and Domokos G., Symbolic dynamics of infinite depth: finding global invariants for BVPs, *Physica D*, 134, 316-336, 1999.

Kocsis A., Buckling Analysis of the Discrete Planar Cosserat Rod, *International Journal of Structural Stability and Dynamics*, 16:(1), 1450111, 1-29, 2016.

Kocsis A., Challamel N. and Károlyi G., Discrete and nonlocal models of Engesser and Haringx *elastica*, *Int. J. Mech. Sc.*, 130, 571-585, 2017.

Kocsis A. and Challamel N., On the foundation of a generalized nonlocal extensible shear beam model from discrete interactions, *Special Issue in honour of Prof. Maugin*, Ed. H. Altenbach, J. Pouget, M. Rousseau, B. Collet and T. Michelitsch, *Generalized Models and Non-classical Approaches in Complex Materials*, Advanced Structured Materials, Springer, 2018.

Koiter W.T., Elastic stability and post-buckling, Proc. Symp. “Nonlinear Problems”, Edited by R.E. Langer, University of Wisconsin Press, 1963.

Koiter W.T., *Elastic stability of solids and structures*, Edited by A.M.A. van der Heijden, Cambridge University Press, 2009.

Massoumi S., Challamel N. and Lerbet J., Exact solutions for the vibration of finite granular beam using discrete and gradient elasticity Cosserat models, *J. Sound Vibration*, 494, 115839, 2021.

McNamara S., Garcia-Rojo R. And Hermann H.J., Microscopic origin of granular ratcheting, *Physical Review E*, 77, 031304, 1-12, 2008.

Navier L., Sur les lois de l'équilibre et du mouvement des corps solides élastiques, *Bulletin des sciences par la Société Philomatique de Paris* pp 177–181, 1823 (in French).

Nicot F., Xiong H., Wautier A., Lerbet J. and Darve F., Force chain collapse as grain column buckling in granular materials, *Granular Matter*, 19, 18, 2017.

Pasternak E. and Mühlhaus H. B., Generalized homogenization procedures for granular materials, *J. Engineering Mathematics*, 51, 1, 199-229, 2005.

Poisson S.D., Mémoire sur l'équilibre et le mouvement des corps élastiques, *Mémoire de l'Académie des Sciences de l'Institut de France*, 8:357–570, 1829 (in French).

Satake M., Finite difference approach to the shear band formation from viewpoint of particle column buckling, In: *Thirteenth Southeast Asian Geotechnical Conference*, Taipei, Taiwan: ROC, 16-20 November1998, 815-818, 1998.

Serrano A.A. and Rodriguez-Ortiz J.M., A contribution to the mechanics of heterogeneous granular media, *Proc. Symp. Plasticity and Soil Mechanics*, Palmer A.C. (Ed.), Cambridge University Engineering Department, pp. 215-227, 13-15 September 1973, Cambridge, 1973.

Thompson J.M.T. and Hunt G.W., *A general theory of elastic stability*, John Wiley & Sons, 1973.

Timoshenko S.P. and Gere J.M., *Theory of Elastic Stability*, McGraw Hill, New York, 2nd edition, 1961.

Tordesillas A. and Muthuswamy M., On the modelling of confined buckling of force chains, *J. Mech. Phys. Solids*, 57, 4, 706-727, 2009.

Tordesillas A., Hunt G. and Shi J., A characteristic length scale in confined elastic buckling of a force chain, *Granular Matter*, 13, 215-218, 2011.

Turco E., dell'Isola F. and Misra A., A nonlinear Lagrangian particle model for grains assemblies including grain relative rotations, *Int. J. Anal. Num. Meth. Geomech.*, 43, 1051-1079, 2019.

Turco E., Barchiesi E., Giorgio I. and Dell'Isola F., A Lagrangian Hencky-type non-linear model suitable for metamaterials design of shearable and extensible slender deformable bodies alternative to Timoshenko theory, *Int. J. Non-linear Mech.*, 123, 103481, 2020.

Vardoulakis I., *Cosserat continuum mechanics with applications to granular media*, Lecture Notes in Applied and Computational Mechanics, Vol. 87, Springer, 2019.

Wang C.Y., Asymptotic formula for the flexible bar, *Mechanism and Machine Theory*, 34, 645-655, 1999.

Wang C.M., Zhang H., Challamel N. and Pan W., *Hencky-Bar-Chain/Net for Structural Analysis*, World Scientific, 2020.

APPENDIX

Appendix A: Solution of the linear difference eigenvalue problem – Some other boundary conditions

In this appendix, we derive the exact buckling formulae of the granular elastica for some other boundary conditions, for instance for clamped-clamped (difference) boundary conditions. The buckling solution is obtained from the resolution of a linear fourth-order difference equation Eq. (35):

$$EI\left(1-\frac{P}{\kappa GA}\right)\delta_2^2 w_i + P\delta_2\delta_0 w_i = 0 \tag{A1}$$

The general solution for the linear difference equation Eq. (A1) can finally be expressed in polynomial and trigonometric functions:

$$w_i = A + iB + C\cos(\varphi i) + D\sin(\varphi i) \quad \text{with} \quad \varphi = \arccos\left[1-\frac{\frac{\beta}{2n^2}}{1-\beta s^2+\frac{\beta}{4n^2}}\right] \tag{A2}$$

Let us investigate the clamped-clamped case based on the following difference boundary conditions (alternative boundary conditions):

$$w_0 = 0\,,\ w_1 = w_{-1}\,,\ w_n = 0 \ \text{and} \ w_{n+1} = w_{n-1} \tag{A3}$$

The consideration of the four boundary conditions Eq. (A3) gives the dimensionless buckling load formula:

$$2-2\cos(n\varphi)-n\sin(\varphi)\sin(n\varphi)=0 \quad \Rightarrow \quad \varphi = \frac{2\pi}{n} \tag{A4}$$

In this case, the buckling load is computed from:

$$\cos\frac{2\pi}{n} = 1 - \frac{\frac{\beta}{2n^2}}{1 - \beta s^2 + \frac{\beta}{4n^2}} \quad \Rightarrow \quad \beta = \frac{4n^2 \sin^2\left(\frac{\pi}{n}\right)}{\cos^2\left(\frac{\pi}{n}\right) + 4s^2 n^2 \sin^2\left(\frac{\pi}{n}\right)} \tag{A5}$$

The buckling load in absence of shear interaction is then equal to:

$$s = 0 \quad \Rightarrow \quad \beta = 4n^2 \tan^2\left(\frac{\pi}{n}\right) \tag{A6}$$

which has been obtained by Satake (1998) – see Eq. (15) of the paper of Satake (1998) expressed with the notation of this paper:

$$k_t = 0 \quad \Rightarrow \quad P = \frac{2C_R}{R}\tan^2\left(\frac{2\pi R}{L}\right) \qquad \text{with} \quad C_R = \frac{EI}{2R},\ k_t = \frac{\kappa GA}{2R} \text{ and}$$

$$s^2 = \frac{EI}{\kappa GAL^2} = \frac{C_R}{k_t L^2} \tag{A7}$$

Appendix B: Analytical solution for *n*=2 (three grains)

The analytical solution for the geometrically exact Engesser granular elastica for three grains (*n*=2) is given below.

The second equation of Eq. (25) for *i*=0,1, with the boundary conditions Eq. (27) and the geometric constraint Eq. (50) yields:

$$\begin{aligned} &2\theta_1 - 2\theta_0 + \frac{\beta}{n^2}\sin\psi_{1/2} = 0 \quad \Rightarrow \quad \theta_1 = \theta_0 - \frac{\beta}{2n^2}\sin\psi_{1/2} \\ &\theta_2 - 2\theta_1 + \theta_0 = 0 \quad \Rightarrow \quad \theta_2 = \theta_0 - \frac{\beta}{n^2}\sin\psi_{1/2} \end{aligned} \tag{B1}$$

The first equation of Eq. (25) for *i*=0,2, considering boundary conditions Eq. (27) is:

$$
\begin{aligned}
&2\theta_1 - 2\theta_0 + \frac{1}{s^2 n^2}\left(\psi_{1/2} - \frac{2\theta_1 + 2\theta_0}{4}\right) = 0 \\
&-2\theta_2 + 2\theta_1 + \frac{1}{s^2 n^2}\left(\psi_{1+1/2} - \frac{2\theta_2 + 2\theta_1}{4}\right) = 0
\end{aligned}
\tag{B2}
$$

Substituting Eq. (B1) in (B2), and eliminating θ_0 yield the equality:

$$
\beta = \frac{2n^2}{1 + 4s^2 n^2} \frac{\psi_{1/2} - \psi_{1+1/2}}{\sin \psi_{1/2}} \tag{B3}
$$

This formula yields Eq. (53) if Eq. (52) is used for $\psi_{1+1/2}$. Eq. (B3) is also equivalently obtained from the application of the single nonlinear difference equation Eq. (29):

$$
\psi_{1+1/2} - \psi_{1/2} - \beta s^2 \left(\sin \psi_{1+1/2} - \sin \psi_{1/2}\right) + \frac{\beta}{4n^2}\left(\sin \psi_{1+1/2} + 3 \sin \psi_{1/2}\right) = 0 \tag{B4}
$$

Using the kinematic constraint Eq. (51) reduces the nonlinear equation Eq. (B4) as:

$$
\psi_{1+1/2} - \psi_{1/2} + 2\beta\left(s^2 + \frac{1}{4n^2}\right) \sin \psi_{1/2} = 0 \tag{B5}
$$

which is equivalent to Eq. (B3). On expresses for the first family of the post-bifurcation branch, using $\psi_{1+1/2} = -\psi_{1/2}$:

$$
\frac{\beta}{\beta_0} = \frac{\psi_{1/2}}{\sin \psi_{1/2}} \quad \text{with} \quad \beta_0 = \frac{4n^2}{1 + 4s^2 n^2} = \frac{16}{1 + 16 s^2} \quad \textit{for } n=2 \tag{B6}
$$

Eq. (B6) can be equivalently reformulated using dimensional quantities (valid for *n=2*):

$$\frac{PR}{C_R}=\frac{2}{1+\dfrac{C_R}{k_t R^2}}\frac{\psi_{1/2}}{\sin\psi_{1/2}} \qquad \text{with} \quad C_R=\frac{EI}{2R}\ ,\ k_t=\frac{\kappa GA}{2R} \text{ and } s^2=\frac{EI}{\kappa GAL^2}=\frac{C_R}{k_t L^2} \tag{B7}$$

Eq. (B6) or Eq. (B7) clearly show that the post-bifurcation path is stable, as also highlighted in Fig. 5. The stability of this post-bifurcation branch can be easily checked from application of Lagrange-Dirichlet theorem of definite positivity of the associated stiffness matrix. The total potential energy of the three-grain system is equal to:

$$\frac{\pi}{a}\left(\theta_0,\theta_1,\theta_2,\psi_{1/2},\psi_{3/2}\right)=\frac{1}{2}\sum_{i=0}^{1}EI\left(\frac{\theta_{i+1}-\theta_i}{a}\right)^2+\frac{1}{2}\sum_{i=0}^{1}\kappa GA\left(\psi_{i+1/2}-\frac{\theta_i+\theta_{i+1}}{2}\right)^2-\sum_{i=0}^{1}P\left[1-\cos\left(\psi_{i+1/2}\right)\right] \tag{B8}$$

which is also expressed, by using $\psi_{1+1/2}=-\psi_{1/2}$ for the first family of equilibrium path, as:

$$\frac{\pi}{a}\left(\theta_0,\theta_1,\theta_2,\psi_{1/2}\right)=\frac{1}{2}EI\left[\left(\frac{\theta_1-\theta_0}{a}\right)^2+\left(\frac{\theta_2-\theta_1}{a}\right)^2\right]+\frac{1}{2}\kappa GA\left[\left(\psi_{1/2}-\frac{\theta_0+\theta_1}{2}\right)^2+\left(\psi_{1/2}+\frac{\theta_1+\theta_2}{2}\right)^2\right]$$
$$-\sum_{i=0}^{1}2P\left[1-\cos\left(\psi_{1/2}\right)\right] \tag{B9}$$

The stationarity of π gives the following nonlinear system for this four-degree-of-freedom system:

$$\begin{cases} -4s^2\left(\theta_1-\theta_0\right)-\dfrac{1}{2}\left(\psi_{1/2}-\dfrac{\theta_0+\theta_1}{2}\right)=0 \\ 4s^2\left(\theta_1-\theta_0\right)-4s^2\left(\theta_2-\theta_1\right)-\dfrac{1}{2}\left(\psi_{1/2}-\dfrac{\theta_0+\theta_1}{2}\right)+\dfrac{1}{2}\left(\psi_{1/2}+\dfrac{\theta_1+\theta_2}{2}\right)=0 \\ 4s^2\left(\theta_2-\theta_1\right)+\dfrac{1}{2}\left(\psi_{1/2}+\dfrac{\theta_1+\theta_2}{2}\right)=0 \\ 2\psi_{1/2}+\dfrac{\theta_2-\theta_0}{2}-2\beta s^2\sin\psi_{1/2}=0 \end{cases} \tag{B10}$$

which implies that:

$$\beta = \frac{16}{1+16s^2}\frac{\psi_{1/2}}{\sin\psi_{1/2}} \quad ;\ \theta_0 = \frac{2}{1+16s^2}\psi_{1/2}\ ;\ \theta_1 = 0\ ;\ \theta_2 = -\theta_0 \quad \text{and} \quad \psi_{1/2} = \arcsin\frac{w_1}{a} \tag{B11}$$

Eq. (B6) is found again from the primary post-bifurcation branch. The determinant of the associated 4×4 stiffness matrix is calculated from:

$$\begin{vmatrix} 4s^2+\frac{1}{4} & -4s^2+\frac{1}{4} & 0 & -\frac{1}{2} \\ -4s^2+\frac{1}{4} & 8s^2+\frac{1}{2} & -4s^2+\frac{1}{4} & 0 \\ 0 & -4s^2+\frac{1}{4} & 4s^2+\frac{1}{4} & \frac{1}{2} \\ -\frac{1}{2} & 0 & \frac{1}{2} & 2-2\beta s^2\cos\psi_{1/2} \end{vmatrix} = 64s^4\left(1-\frac{\beta}{\beta_0}\cos\psi_{1/2}\right) = 64s^4\left(1-\frac{\psi_{1/2}}{\tan\psi_{1/2}}\right) \tag{B12}$$

Sylvester's criterion can be applied for checking the stability of the primary post-bifurcation path.

There is a bifurcation at the specific point $\left(\psi_{1/2}=\frac{\pi}{2}, \beta=\frac{\pi}{2}\beta_0\right)$. The branch intersecting the primary branch is a rigid rotation mechanism (the structure becomes kinematically indeterminate) which corresponds to the superposition of grain 2 with grain 0. The stiffness matrix is degenerate for this second bifurcation branch.

$$\begin{pmatrix} 4s^2+\frac{1}{4} & -4s^2+\frac{1}{4} & 0 & -\frac{1}{2} \\ -4s^2+\frac{1}{4} & 8s^2+\frac{1}{2} & -4s^2+\frac{1}{4} & -1 \\ 0 & -4s^2+\frac{1}{4} & 4s^2+\frac{1}{4} & -\frac{1}{2} \\ -\frac{1}{2} & -1 & -\frac{1}{2} & 2 \end{pmatrix} \begin{pmatrix} \theta_0 \\ \theta_0 \\ \theta_0 \\ \psi_{1/2} \end{pmatrix} = \begin{pmatrix} 0 \\ -\frac{\pi}{2} \\ -\frac{\pi}{2} \\ \pi \end{pmatrix} \tag{B13}$$

This phenomenon is very similar to what is observed by Károlyi and Domokos (1999) for the geometrically exact analysis of Hencky system with two rigid links ($n=2$) (where the primary bifurcation branch is also intersected by a branch with rigid body motion). In the present granular case, we have for this specific branch:

$$\theta_0 = \psi_{1/2} - \left(\frac{4s^2 - \frac{1}{4}}{4s^2 + \frac{1}{4}} \right) \frac{\pi}{2};\ \theta_1 = \psi_{1/2} - \frac{\pi}{2};\ \theta_2 = \psi_{1/2} - \left(\frac{4s^2 + \frac{3}{4}}{4s^2 + \frac{1}{4}} \right) \frac{\pi}{2} \tag{B14}$$

It is worth mentioning that the interpenetration condition between rigid grains has not been included in the model. If a non-interpenetration condition between grain 0 and grain 2 is explicitly considered, an additional kinematics constraint has to be taken into account:

$$a\left(\cos\psi_{1/2} + \cos\psi_{1+1/2}\right) = 2a\cos\psi_{1/2} \geq a \quad \Rightarrow \quad \psi_{1/2} \leq \frac{\pi}{3} \tag{B15}$$

The stiffness matrix is definite positive for the stable primary bifurcation path, according to the positive sign of the determinant and the sub-determinants calculated from Eq. (B12). The primary bifurcation branch may evolve until the contact between the two extreme grains of the granular column, if we take this kinematics constraint into account.

It is worth mentioning that the numerical approach does not incorporate a non-interpenetration condition between the rigid grains.

Appendix C: Analytical solution for *n*=3 (four grains)

The analytical solution Eq. (58) for the geometrically exact Engesser granular elastica for four grains (n=3) is detailed below.

The second equation of Eq. (25) for i=0,1,2, with the boundary conditions Eq. (27) and the geometric constraint Eq. (54) yields:

$$\begin{aligned} &2\theta_1 - 2\theta_0 + \frac{\beta}{n^2}\sin\psi_{1/2} = 0 \quad \Rightarrow \quad \theta_1 = \theta_0 - \frac{\beta}{2n^2}\sin\psi_{1/2} \\ &\theta_2 - 2\theta_1 + \theta_0 - \frac{\beta}{n^2}\sin\psi_{1/2} = 0 \quad \Rightarrow \quad \theta_2 = \theta_1 \\ &\theta_3 - 2\theta_2 + \theta_1 - \frac{\beta}{n^2}\sin\psi_{1/2} = 0 \quad \Rightarrow \quad \theta_3 = \theta_0 \end{aligned} \tag{C1}$$

The first equation of Eq. (25) for i=0,1, considering boundary conditions Eq. (27) and Eq. (C1) leads to:

$$\begin{aligned} &-\frac{\beta}{n^2}\sin\psi_{1/2} + \frac{1}{s^2n^2}\left(\psi_{1/2} - \theta_0 + \frac{\beta}{4n^2}\sin\psi_{1/2}\right) = 0 \\ &\frac{\beta}{2n^2}\sin\psi_{1/2} + \frac{1}{s^2n^2}\left(\frac{\psi_{1/2} + \psi_{1+1/2}}{2} - \theta_0 + \frac{3\beta}{8n^2}\sin\psi_{1/2}\right) = 0 \end{aligned} \tag{C2}$$

Eliminating θ_0 gives:

$$\beta = \frac{4n^2}{1+12s^2n^2}\frac{\psi_{1/2} - \psi_{1+1/2}}{\sin\psi_{1/2}} \tag{C3}$$

From Eq. (57), we can write $\arcsin(2\sin\psi_{1/2}) = -\psi_{1+1/2}$, but in this way we can only account for solutions with $-\pi/2 \le \psi_{1+1/2} \le \pi/2$. To recover solutions beyond this, we need to write: where

$$-\psi_{1+1/2} = \begin{cases} \arcsin(2\sin\psi_{1/2}) - 2k\pi & \text{if} \quad \mathrm{mod}(|\psi_{1+1/2}|, 2\pi) < \dfrac{\pi}{2} \\ \pi - \arcsin(2\sin\psi_{1/2}) + 2k\pi & \text{otherwise} \end{cases} \tag{C4}$$

Eq. (C3) and (C4) lead to Eq. (58).

Note that the non-interpenetration condition for the $n=3$-granular column would be formulated from the angle inequality:

$$\psi_{1/2} \leq \frac{\pi}{2} \tag{C5}$$

Appendix D: Approximation of the post-bifurcation path

An asymptotic expansion of the post-bifurcation branches of the granular *elastica* difference equation is presented in this Appendix, for n larger than *3*. The second-order nonlinear difference eigenvalue problem is governed by Eq. (29):

$$\psi_{i+1} - 2\psi_i + \psi_{i-1} - \beta s^2 \left(\sin\psi_{i+1} - 2\sin\psi_i + \sin\psi_{i-1}\right) + \frac{\beta}{4n^2}\left(\sin\psi_{i+1} + 2\sin\psi_i + \sin\psi_{i-1}\right) = 0 \tag{D1}$$

with the boundary conditions:

$$\psi_{1/2} = \psi_{-1/2} \quad \text{and} \quad \psi_{n-1/2} = \psi_{n+1/2} \tag{D2}$$

We will follow a methodology generally applied to nonlinear continuous stability problems (governed by nonlinear differential or partial differential equations), based on asymptotic expansion of both the kinematic state variable and the load (see Koiter, 1963; see also Koiter, 2009 or Thompson and Hunt, 1973; Wang, 1999). The same asymptotic procedure has been applied as well for nonlinear discrete stability problems governed by nonlinear difference equations (Challamel et al, 2015-a). Challamel et al (2015-a) obtained an asymptotic formula for the primary bifurcation branch of the discrete elastica, which is based on a geometrically exact analysis of Hencky structural system.

The Taylor asymptotic expansion is assumed for both the load and the rotation:

$$\begin{cases} \beta = \beta_0 + \varepsilon\beta_1 + \varepsilon^2\beta_2 + \varepsilon^3\beta_3 + ... \\ \psi_i = \psi_i^{(0)} + \varepsilon\psi_i^{(1)} + \varepsilon^2\psi_i^{(2)} + \varepsilon^3\psi_i^{(3)} + ... \end{cases} \text{and } \varepsilon = \psi_0 \tag{D3}$$

where ε is a small parameter related to the amplitude of the post-buckling behavior. The fundamental path of the granular *elastica* has no prebuckling rotation $\psi_i^{(0)} = 0$. Furthermore, for symmetrical reasons, some terms of the asymptotic expansion vanish, leading to the third-order asymptotic expansion:

$$\begin{cases} \beta = \beta_0 + \varepsilon^2 \beta_2 + ... \\ \psi_i = \varepsilon \psi_i^{(1)} + \varepsilon^3 \psi_i^{(3)} + ... \end{cases} \tag{D4}$$

By inserting this asymptotic expansion in the nonlinear difference equation Eq. (D1) and considering the first and third powers of the small parameter ε, one obtains the following system of two linear second-order difference equations:

$$\begin{cases} \psi_{i+1}^{(1)} - 2\psi_i^{(1)} + \psi_{i-1}^{(1)} - \beta_0 s^2 \left[\psi_{i+1}^{(1)} - 2\psi_i^{(1)} + \psi_{i-1}^{(1)}\right] + \dfrac{\beta_0}{4n^2}\left[\psi_{i+1}^{(1)} + 2\psi_i^{(1)} + \psi_{i-1}^{(1)}\right] = 0 \\ \psi_{i+1}^{(3)} - 2\psi_i^{(3)} + \psi_{i-1}^{(3)} - \beta_0 s^2 \left[\psi_{i+1}^{(3)} - 2\psi_i^{(3)} + \psi_{i-1}^{(3)}\right] + \dfrac{\beta_0}{4n^2}\left[\psi_{i+1}^{(3)} + 2\psi_i^{(3)} + \psi_{i-1}^{(3)}\right] = \\ -\dfrac{\beta_0 s^2}{6}\left[\left(\psi_{i+1}^{(1)}\right)^3 - 2\left(\psi_i^{(1)}\right)^3 + \left(\psi_{i-1}^{(1)}\right)^3\right] + \beta_2 s^2 \left[\psi_{i+1}^{(1)} - 2\psi_i^{(1)} + \psi_{i-1}^{(1)}\right] \\ + \dfrac{\beta_0}{24n^2}\left[\left(\psi_{i+1}^{(1)}\right)^3 + 2\left(\psi_i^{(1)}\right)^3 + \left(\psi_{i-1}^{(1)}\right)^3\right] - \dfrac{\beta_2}{4n^2}\left[\psi_{i+1}^{(1)} + 2\psi_i^{(1)} + \psi_{i-1}^{(1)}\right] \end{cases} \tag{D5}$$

The following normalization procedure is used, as for the difference eigenvalue problem:

$$\psi_0^{(1)} = 1 \text{ and } \psi_0^{(i)} = 0 \text{ for } i \geq 2 \tag{D6}$$

The first difference equation Eq. (D5) has been already solved and gives the linearized fundamental buckling mode:

$$\psi_i^{(1)} = \cos\left(\pi \frac{i}{n}\right) \text{ with } \beta_0 = \frac{4n^2 \sin^2\left(\dfrac{\pi}{2n}\right)}{\cos^2\left(\dfrac{\pi}{2n}\right) + 4s^2 n^2 \sin^2\left(\dfrac{\pi}{2n}\right)} \tag{D7}$$

The substitution of this first-order buckling mode into the second difference equation Eq. (D5) furnishes

$$\psi_{i+1}^{(3)}-2\psi_i^{(3)}+\psi_{i-1}^{(3)}-\beta_0 s^2\left[\psi_{i+1}^{(3)}-2\psi_i^{(3)}+\psi_{i-1}^{(3)}\right]+\frac{\beta_0}{4n^2}\left[\psi_{i+1}^{(3)}+2\psi_i^{(3)}+\psi_{i-1}^{(3)}\right]=$$
$$\frac{1}{n^2}\left(-\beta_2+\frac{\beta_0}{8}\right)\cos\left(\frac{\pi i}{n}\right)\left[\cos^2\left(\frac{\pi}{2n}\right)+4n^2s^2\sin^2\left(\frac{\pi}{2n}\right)\right] \qquad \text{(D8)}$$
$$+\frac{\beta_0}{24n^2}\cos\left(\frac{3\pi i}{n}\right)\left[\cos^2\left(\frac{3\pi}{2n}\right)+4n^2s^2\sin^2\left(\frac{3\pi}{2n}\right)\right]$$

The third order function $\psi_i^{(3)}$ in the asymptotic expansion is then obtained from introduction of the boundary conditions Eq. (D2) and the normalization condition Eq. (D6) in the resolution of Eq. (D8):

$$\psi_i^{(3)}=\frac{\sin^2\left(\frac{\pi}{2n}\right)}{12}\left[\cos^2\left(\frac{3\pi}{2n}\right)+4n^2s^2\sin^2\left(\frac{3\pi}{2n}\right)\right]\frac{\cos\left(\frac{3\pi i}{n}\right)-\cos\left(\frac{\pi i}{n}\right)}{\cos\left(\frac{3\pi}{n}\right)-\cos\left(\frac{\pi}{n}\right)} \quad \text{for } n\neq 2 \qquad \text{(D9)}$$

and the corresponding second-order buckling load factor β_2 is calculated by vanishing the term in $\cos(\pi i/n)$ in Eq. (D8):

$$\beta_2=\frac{\beta_0}{8}=\frac{\frac{n^2}{2}\sin^2\left(\frac{\pi}{2n}\right)}{\cos^2\left(\frac{\pi}{2n}\right)+4s^2n^2\sin^2\left(\frac{\pi}{2n}\right)} \text{ for } n\neq 2 \qquad \text{(D10)}$$

For $n\neq 2$, the asymptotic expansion of the primary post-buckling branch writes for the first terms:

$$\frac{\beta}{\beta_0}=1+\frac{\psi_0^2}{8}+\ldots \qquad \text{with } \beta_0=\frac{4n^2\sin^2\left(\frac{\pi}{2n}\right)}{\cos^2\left(\frac{\pi}{2n}\right)+4s^2n^2\sin^2\left(\frac{\pi}{2n}\right)} \qquad \text{(D11)}$$

We also have from Eq. (D4):

$$\psi_{1/2} = \varepsilon\psi_{1/2}^{(1)} + \varepsilon^3\psi_{1/2}^{(3)} + \ldots \tag{D12}$$

which means that the asymptotic expansion can be also reformulated using the parameter $\psi_{1/2}$, and for $n \neq 2$, as:

$$\frac{\beta}{\beta_0} = 1 + \frac{\psi_{1/2}^2}{8\cos^2\left(\frac{\pi}{2n}\right)} + \ldots \qquad \text{with } \beta_0 = \frac{4n^2\sin^2\left(\frac{\pi}{2n}\right)}{\cos^2\left(\frac{\pi}{2n}\right) + 4s^2n^2\sin^2\left(\frac{\pi}{2n}\right)} \tag{D13}$$

Eq. (D13) is Eq. (61) of the paper.

Appendix E: Reduction of the governing equations

The derivation of Eq. (63) is given below.

Let us express $\psi_{i+1/2}$ from the first equation of Eq. (25)

$$\psi_{i+1/2} = 2s^2n^2(-\theta_{i+1} + 2\theta_i - \theta_{i-1}) + \frac{\theta_{i+1} + 2\theta_i + \theta_{i-1}}{2} - \psi_{i-1/2} \tag{E1}$$

Using boundary conditions $\psi_{1/2} = \psi_{-1/2}$ and $\theta_1 = \theta_{-1}$ from Eq. (27), Eq. (E1) for i =0 yields:

$$\psi_{1/2} = 2s^2n^2(-\theta_1 + \theta_0) + \frac{\theta_1 + \theta_0}{2} \tag{E2}$$

Now we can iterate Eq. (E1):

$$\begin{aligned}
\psi_{1+1/2} &= 2s^2n^2(-\theta_2 + 2\theta_1 - \theta_0) - 2s^2n^2(-\theta_1 + \theta_0) + \frac{\theta_2 + \theta_1}{2} \\
\psi_{2+1/2} &= 2s^2n^2(-\theta_3 + 2\theta_2 - \theta_1) - 2s^2n^2(-\theta_2 + 2\theta_1 - \theta_0) + 2s^2n^2(-\theta_1 + \theta_0) + \frac{\theta_3 + \theta_2}{2} \\
\psi_{3+1/2} &= 2s^2n^2(-\theta_4 + 2\theta_3 - \theta_2) - 2s^2n^2(-\theta_3 + 2\theta_2 - \theta_1) + 2s^2n^2(-\theta_2 + 2\theta_1 - \theta_0) - \\
&- 2s^2n^2(-\theta_1 + \theta_0) + \frac{\theta_4 + \theta_3}{2}
\end{aligned} \tag{E3}$$

which can be generalized as Eq. (62).

To verify the formula let i be i-1 in Eq. (62) :

$$\psi_{i-1/2} = 2s^2n^2\left((-1)^{i-1}(-\theta_1+\theta_0)+\sum_{j=1}^{i-1}(-1)^{i-1-j}(-\theta_{j+1}+2\theta_j-\theta_{j-1})\right)+\frac{\theta_i+\theta_{i-1}}{2}$$

Now we add the above equation to Eq. (62):

$$\psi_{i+1/2}+\psi_{i-1/2} = 2s^2n^2(-\theta_{i+1}+2\theta_i-\theta_{i-1})+\frac{\theta_{i+1}+2\theta_i+\theta_{i-1}}{2}$$

This is consistent with the first equation of Eq. (25).

Note that in the numerics only Eq. (E1) and (E2) are used.

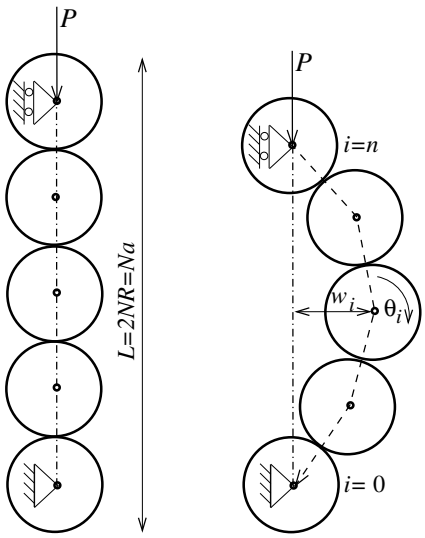

Figure 1. The mechanical model of the *granular elastica*

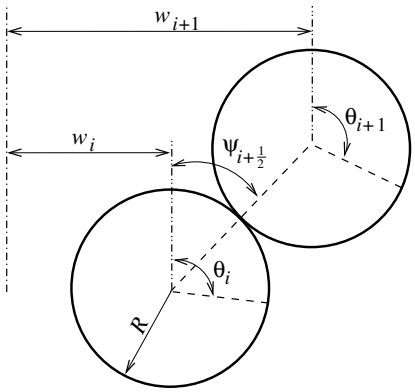

Figure 2. Schematic of two neighboring discs after deformation of the structure

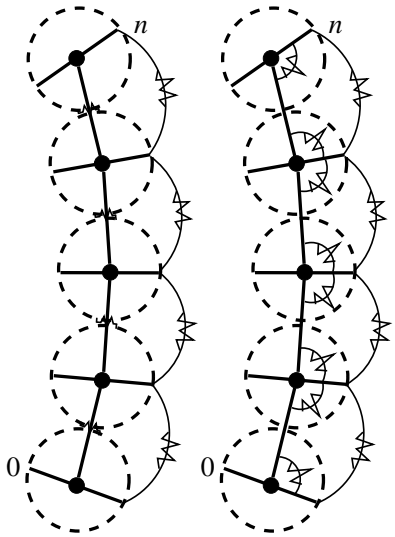

Figure 3. Two equivalent DEM granular models, without lateral support spring, based on shear and rotational granular interactions. The model on the left is equipped with a linear spring of stiffness C_R against relative rotations and a linear spring of stiffness k_t against relative tangential motions (slip) (DEM model - Serrano and Rodriguez-Ortiz, 1973; Cundall and Strack, 1979 or more recently Hunt et al, 2010), while the model on the right is equipped with bending and shear rotational springs.

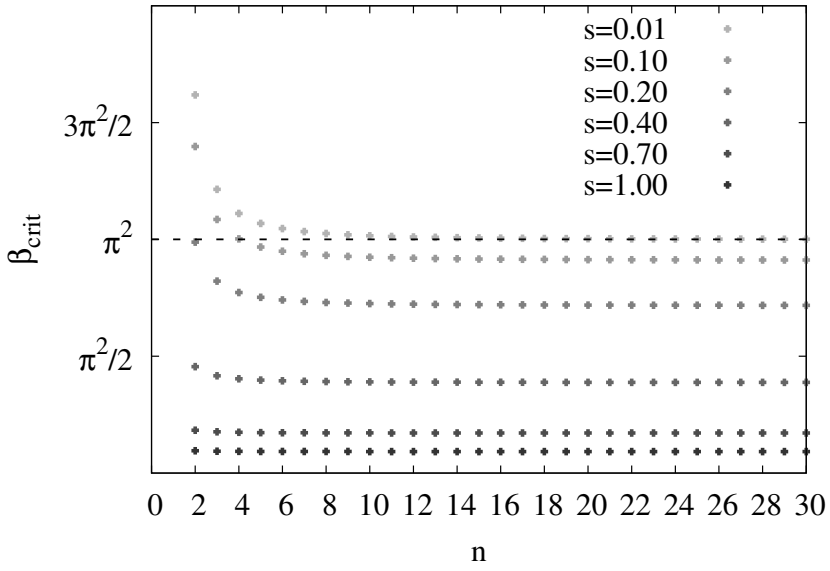

Figure 4. Buckling load parameter as function of *n* for various stiffness parameter values *s*

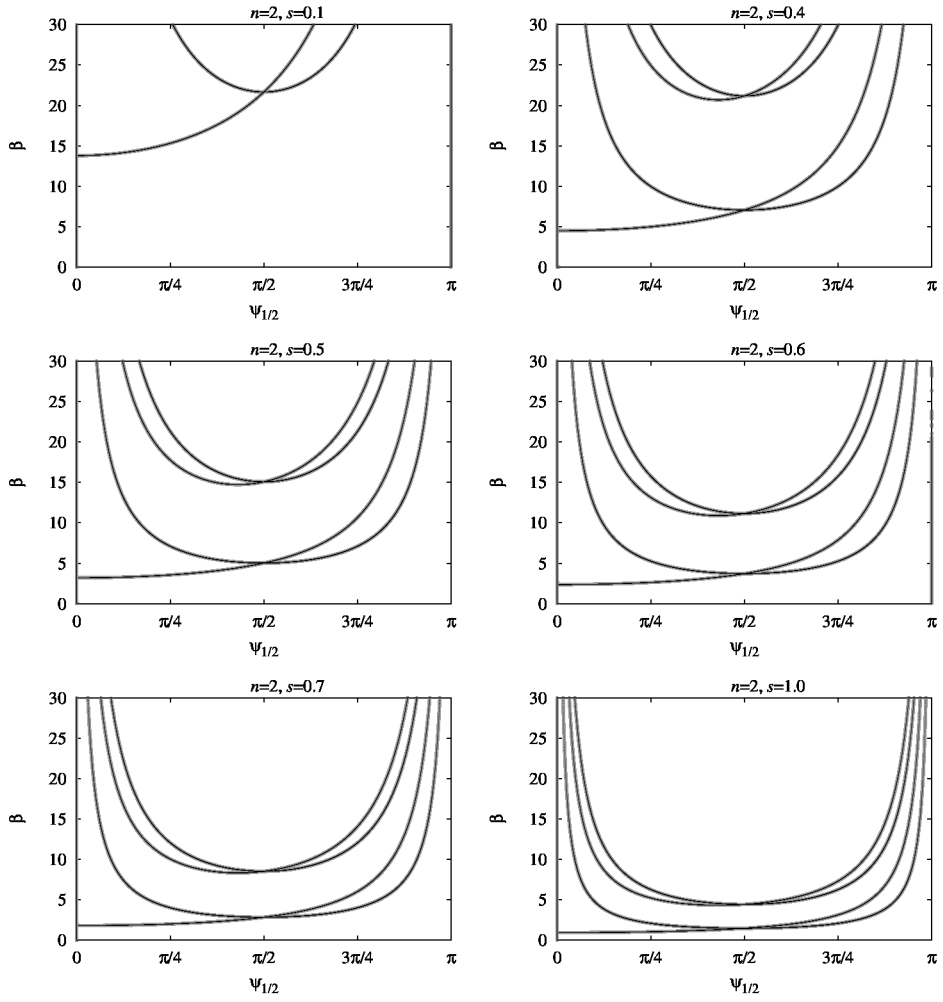

Figure 5. Equilibrium paths of three grains (n=2) wiht various values of the stiffness parameter s from numerical simulation (grey). Identical analytical results given by Eq. (53) for the same stiffness parameters as validation of the numerical solutions (black dots). Numerical results are based on scanning the bounded domain $\theta_0 \in [0,\pi]$, $\theta_1, \theta_2 \in [-2\pi, 2\pi]$ and $\beta \in (0,30]$.

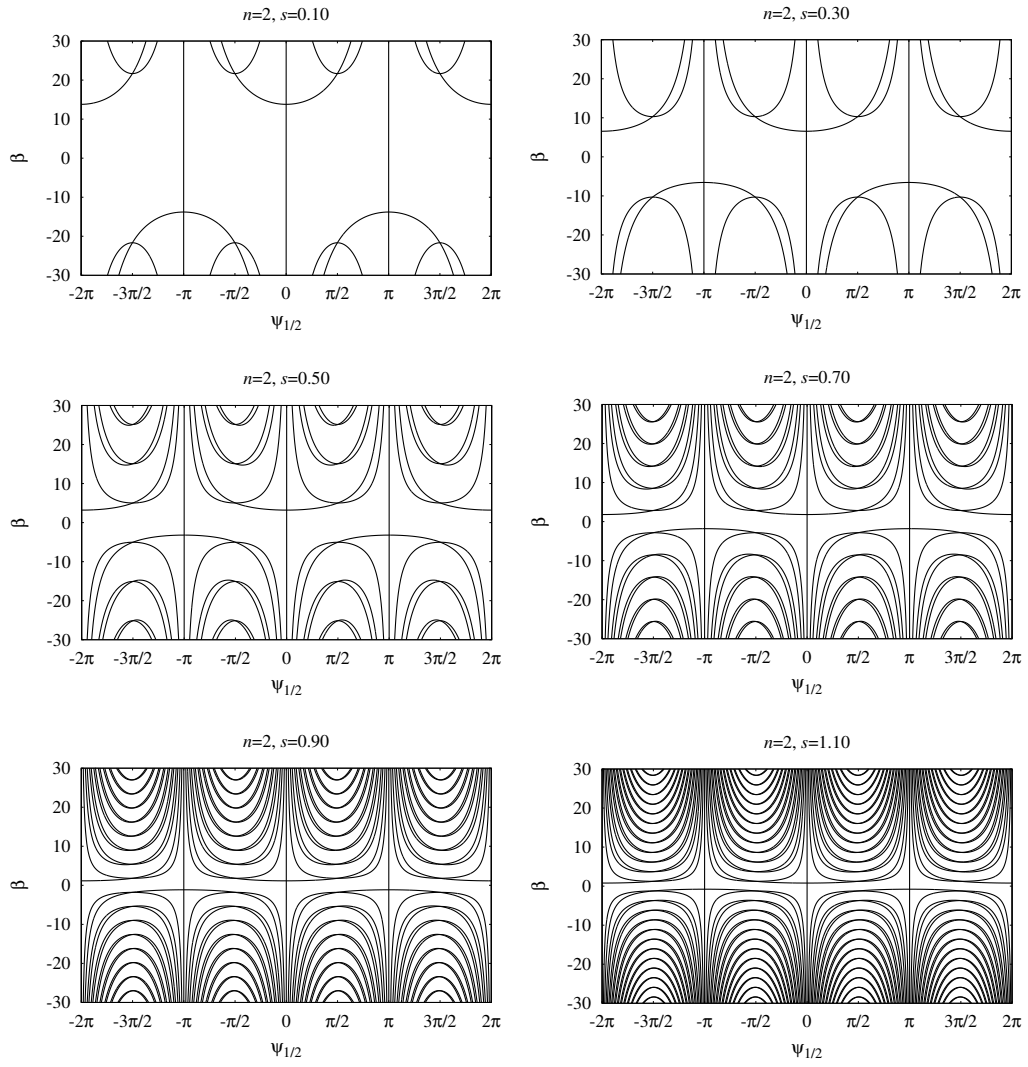

Figure 6. All the equilibrium paths of the granuar elastica of three grains (n=2) in the bounded domain of the load parameter $\beta \in [-30,30]$ with various values of the stiffness parameter s based on analytical results given by Eq. (53).

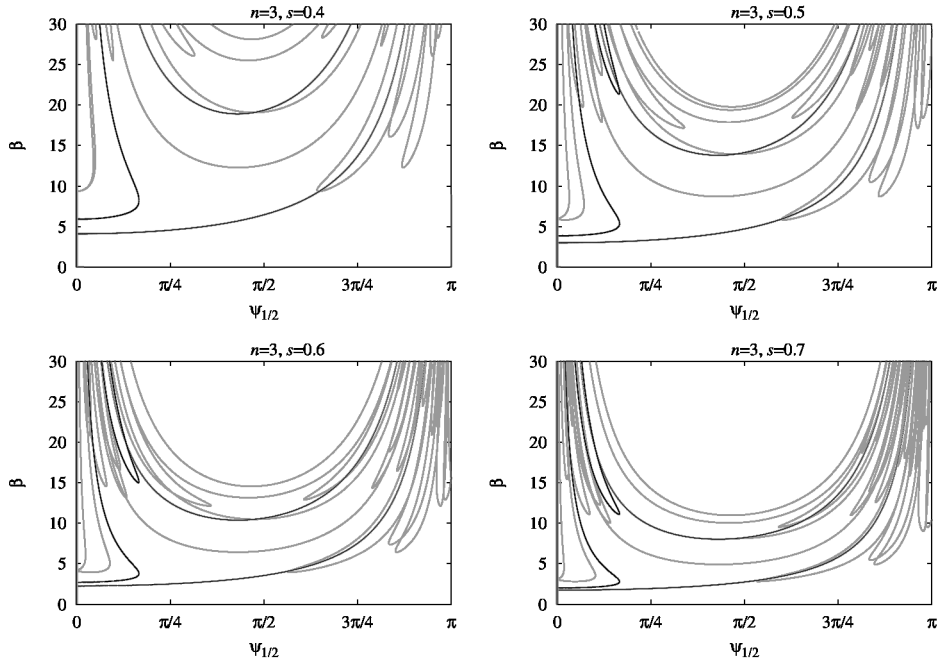

Figure 7. Equilibrium paths of four grains (n=3) with various values of the stiffness parameter s from numerical simulation (grey). Analytical results for symmetric configurations given by Eq. (56) and (58) for the same stiffness parameters as validation of the numerical solutions (black dots). Numerical results are based on scanning the bounded domain $\theta_0 \in [0,\pi]$, $\theta_1,\theta_2,\theta_3 \in [-2\pi,2\pi]$ and $\beta \in (0,30]$.

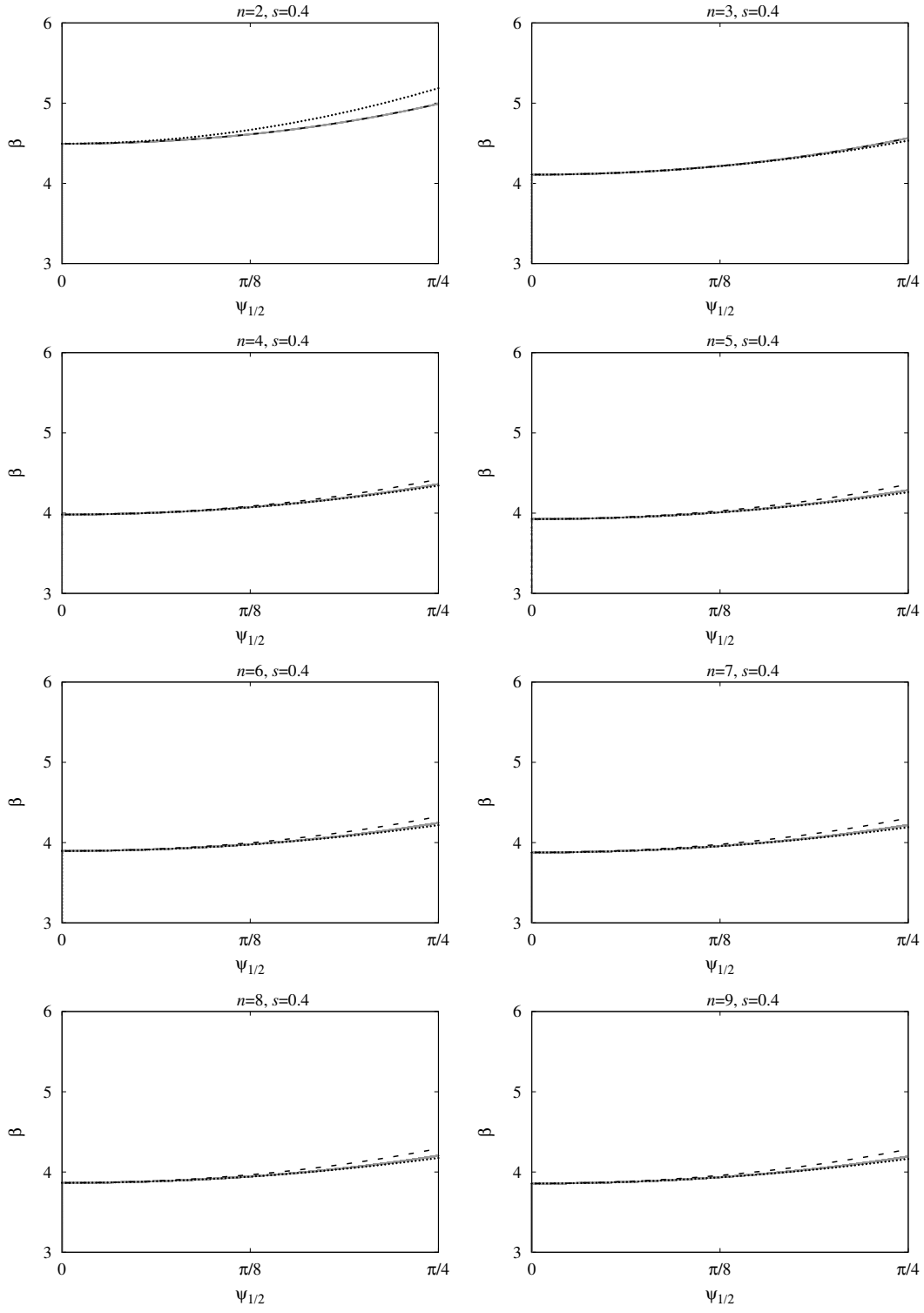

Figure 8. Numerical simulation results for the first post-buckling path with various number n of grains for stiffness parameter s=0.4 (grey). Approximate analytical results given by Eq. (60) (black dashed line) and by Eq. (61) (black dotted line) are also shown.

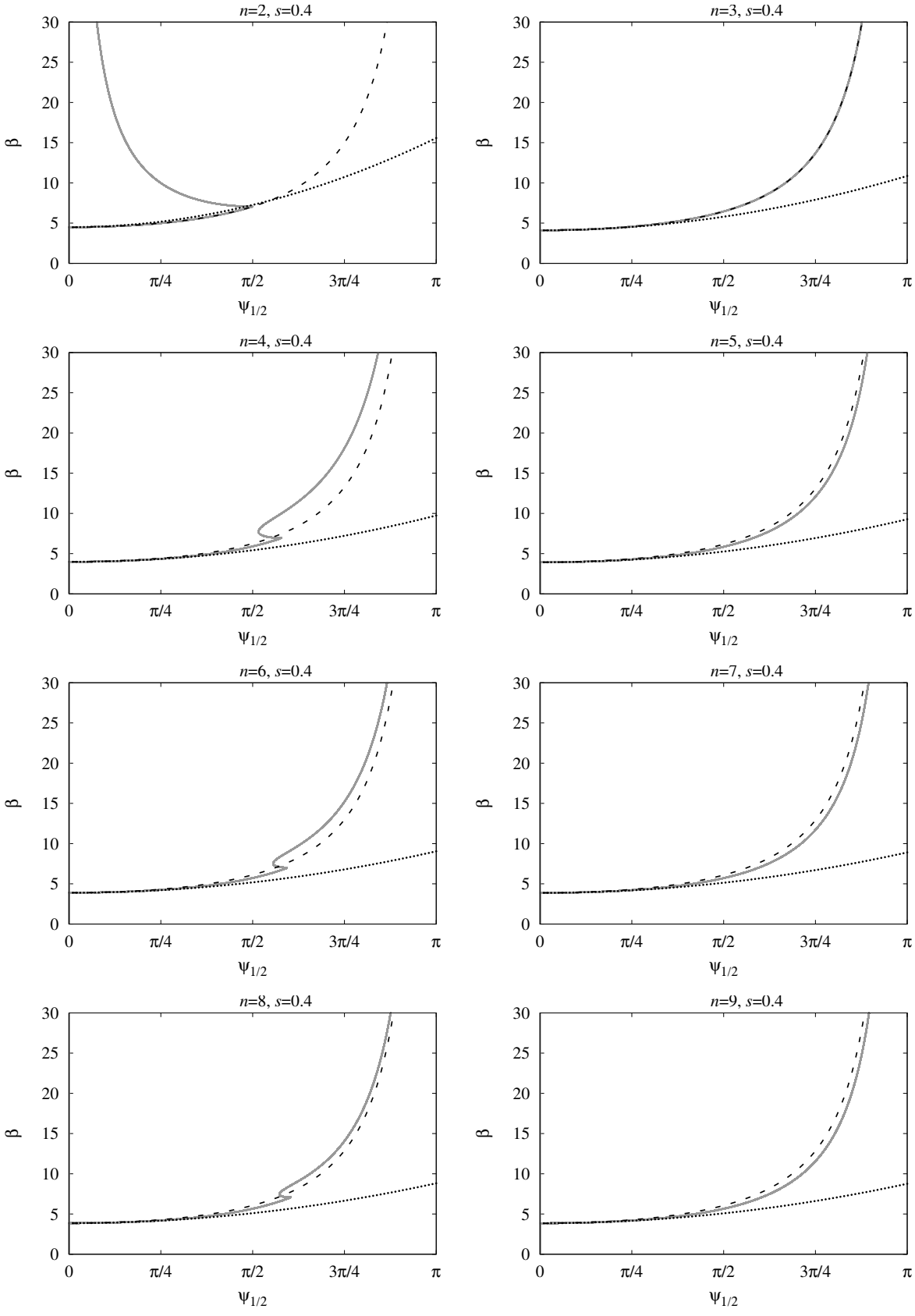
n=2, s=0.4
n=3, s=0.4
n=4, s=0.4
n=5, s=0.4
n=6, s=0.4
n=7, s=0.4
n=8, s=0.4
n=9, s=0.4
β
ψ1/2
0
π/4
π/2
3π/4
π
5
10
15
20
25
30

Figure 9. Numerical simulation results for the first post-buckling path with various number n of grains for stiffness parameter s=0.4 (grey). Approximate analytical results given by Eq. (60) (black dashed line) and by Eq. (61) (black dotted line) are also shown.